



April 24 - 27, 2023
JMS Aster Plaza, Hiroshima, Japan



Probing jet transport coefficient of cold nuclear matter in electron-ion collisions

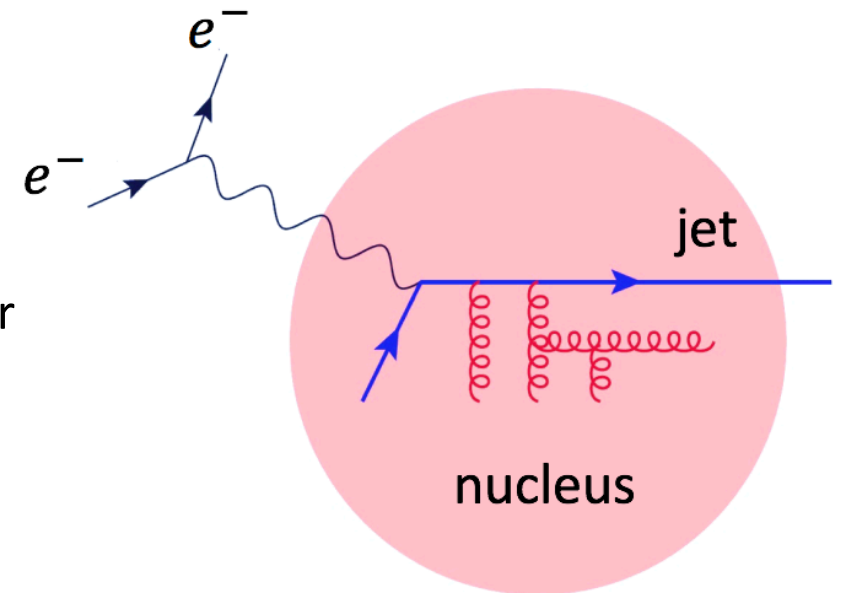
Peng Ru / 茹芃



School of Materials and New Energy & Institute of Quantum Matter
South China Normal University

In collaboration with:

Zhong-Bo Kang, Enke Wang, Hongxi Xing, Ben-Wei Zhang



Outline

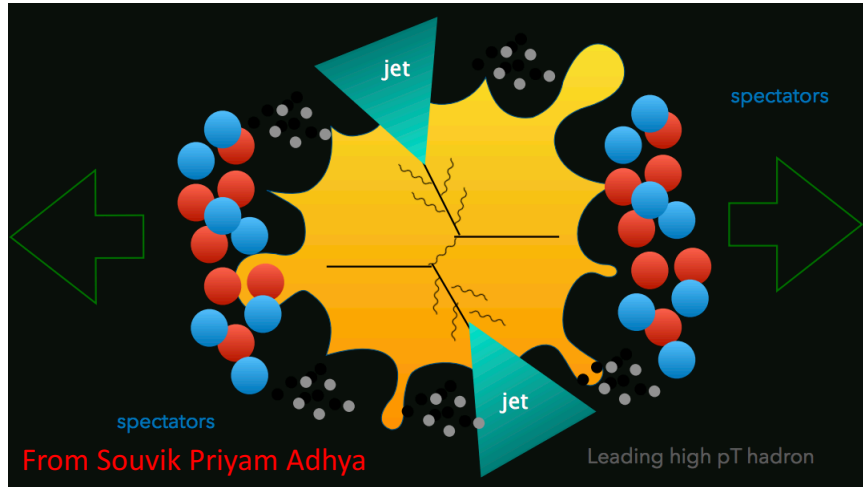
1.
Motivation

2. Kinematics dependent \hat{q}
within high-twist factorization

3. Transverse momentum
broadening/imbalance in
electron-ion collisions

4.
Summary

Jet quenching in heavy-ion collisions



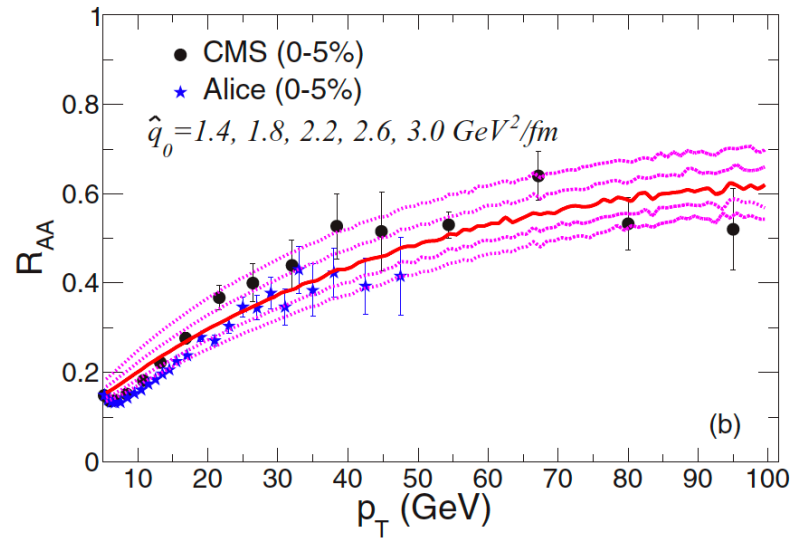
\hat{q} is an important **non-perturbative** input in jet-quenching models.

Transverse momentum broadening per unit length for propagating parton.

Characterize **interaction strength** between hard probe and nuclear medium.

Jet quenching in heavy-ion collisions

JET, PRC 90, 014909 (2014)

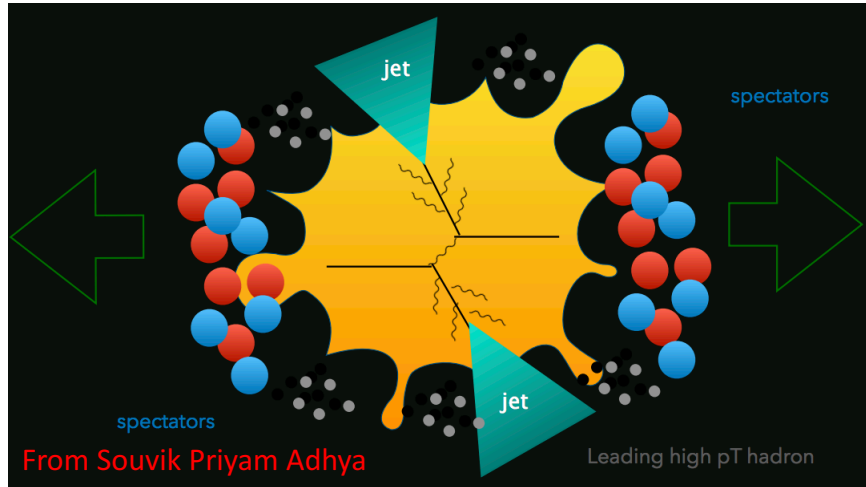


\hat{q} is an important **non-perturbative** input in jet-quenching models.

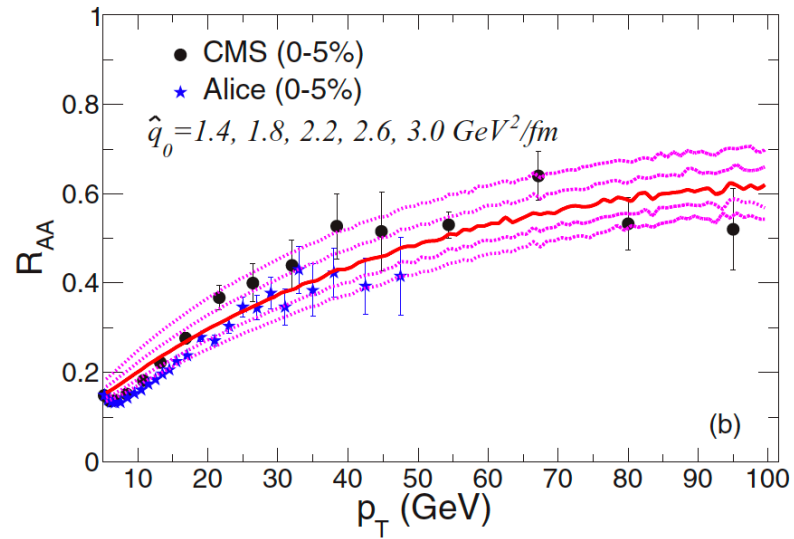
Transverse momentum broadening per unit length for propagating parton.

Characterize **interaction strength** between hard probe and nuclear medium.

Jet quenching in heavy-ion collisions



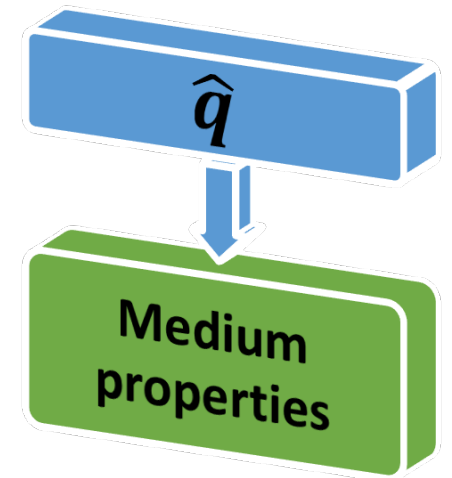
JET, PRC 90, 014909 (2014)



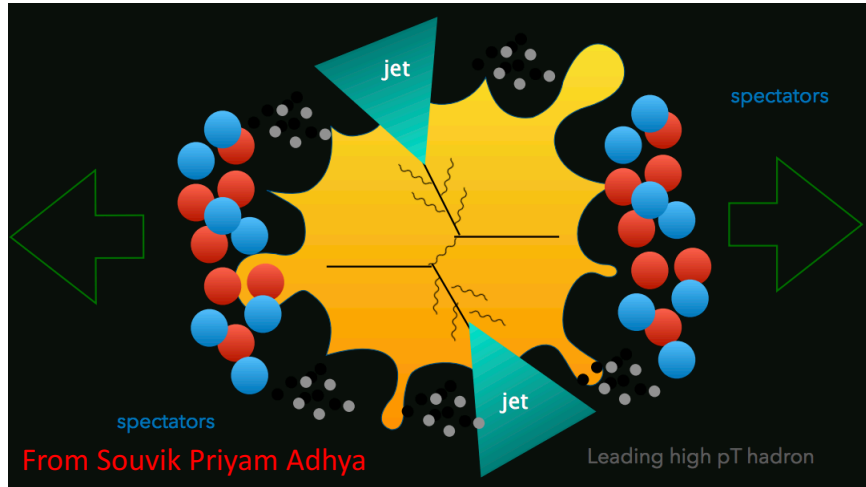
\hat{q} is an important **non-perturbative** input in jet-quenching models.

Transverse momentum broadening per unit length for propagating parton.

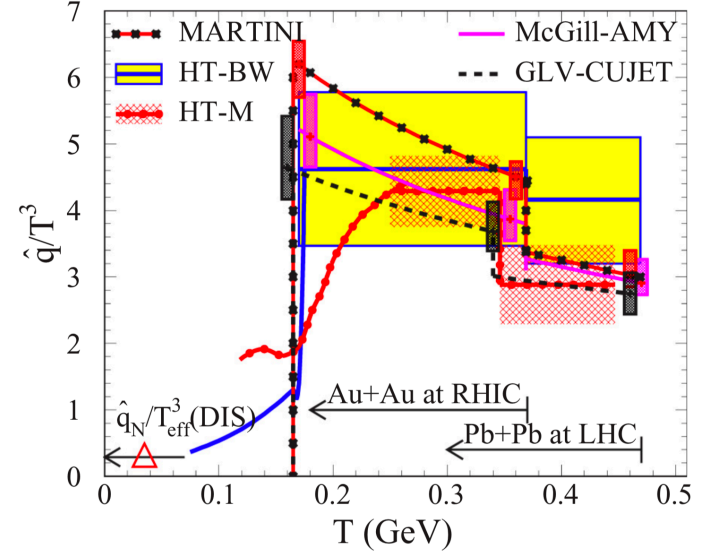
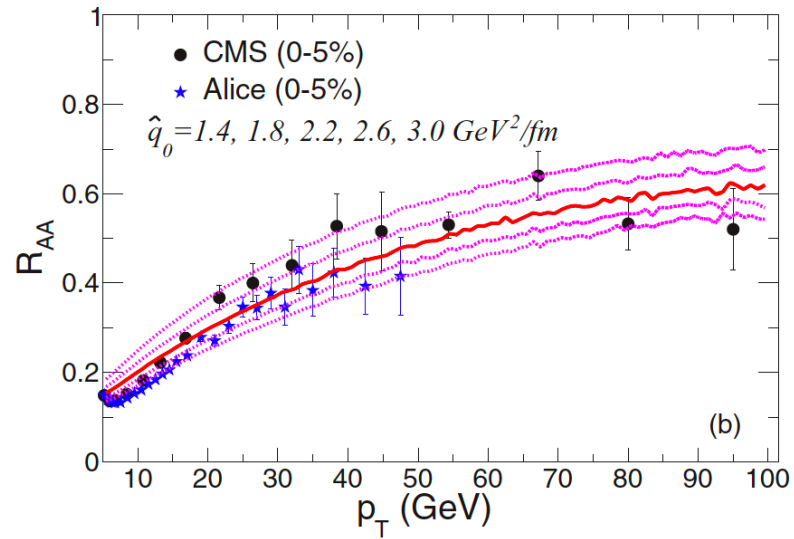
Characterize **interaction strength** between hard probe and nuclear medium.



Jet quenching in heavy-ion collisions



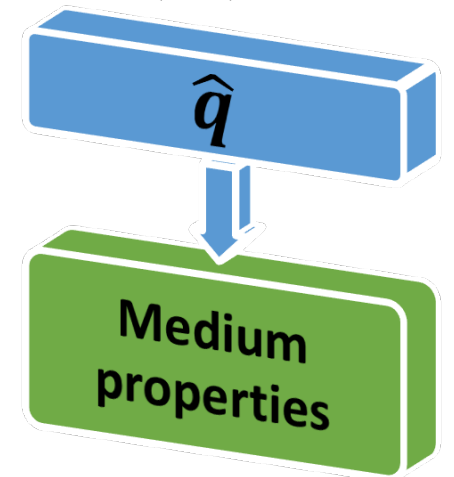
JET, PRC 90, 014909 (2014)



\hat{q} is an important **non-perturbative** input in jet-quenching models.

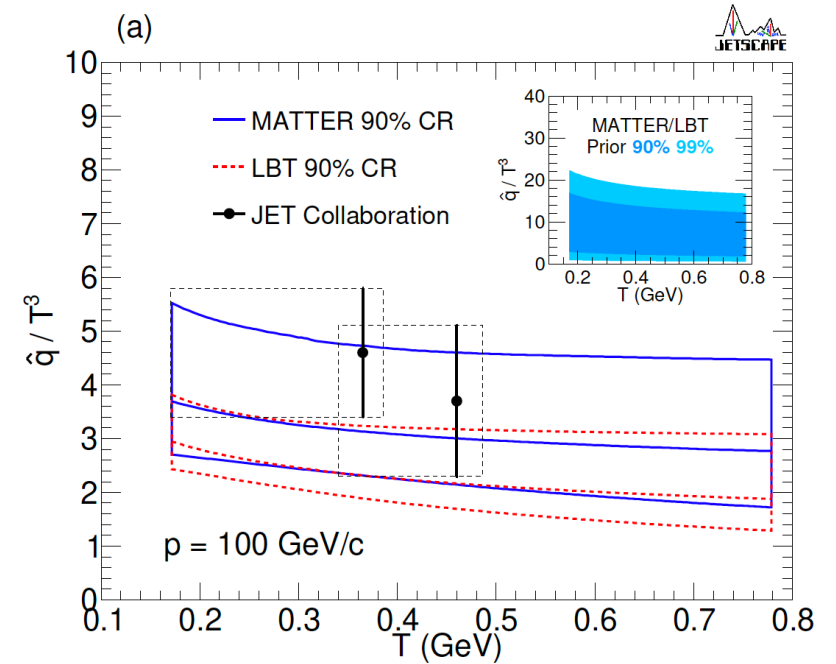
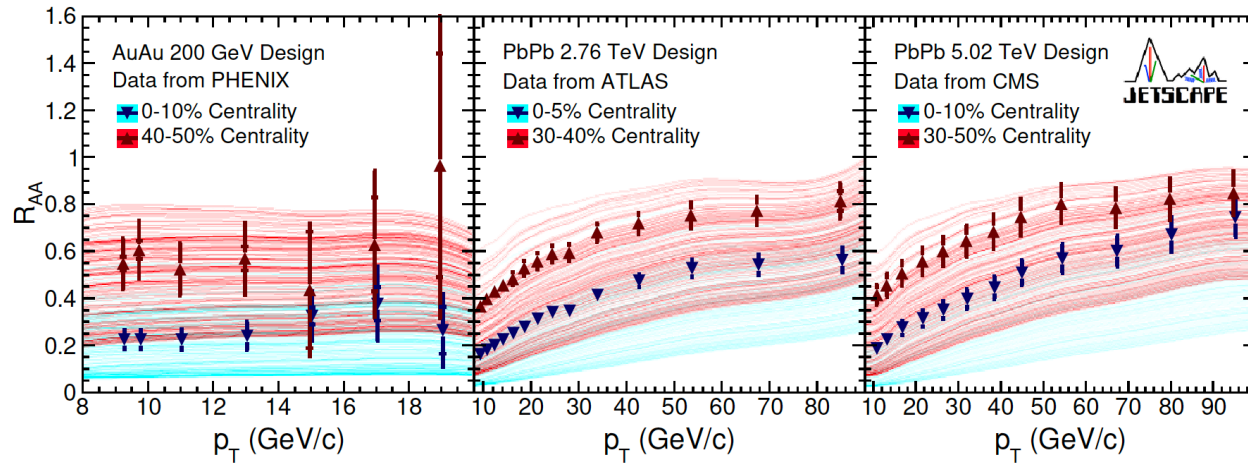
Transverse momentum broadening per unit length for propagating parton.

Characterize **interaction strength** between hard probe and nuclear medium.



Temperature dependence of \hat{q} from Bayesian analysis

JETSCAPE, PRC **104**, 024905 (2021)

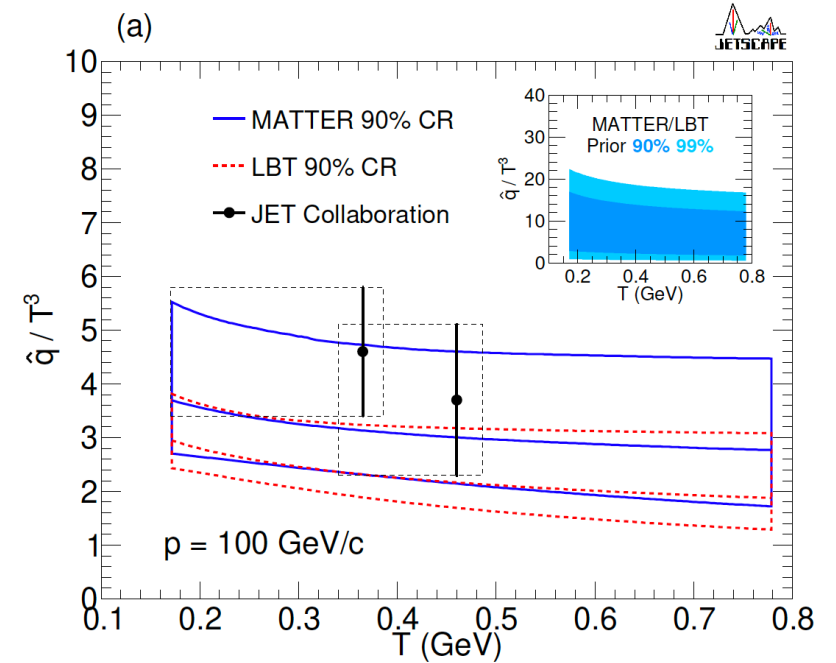
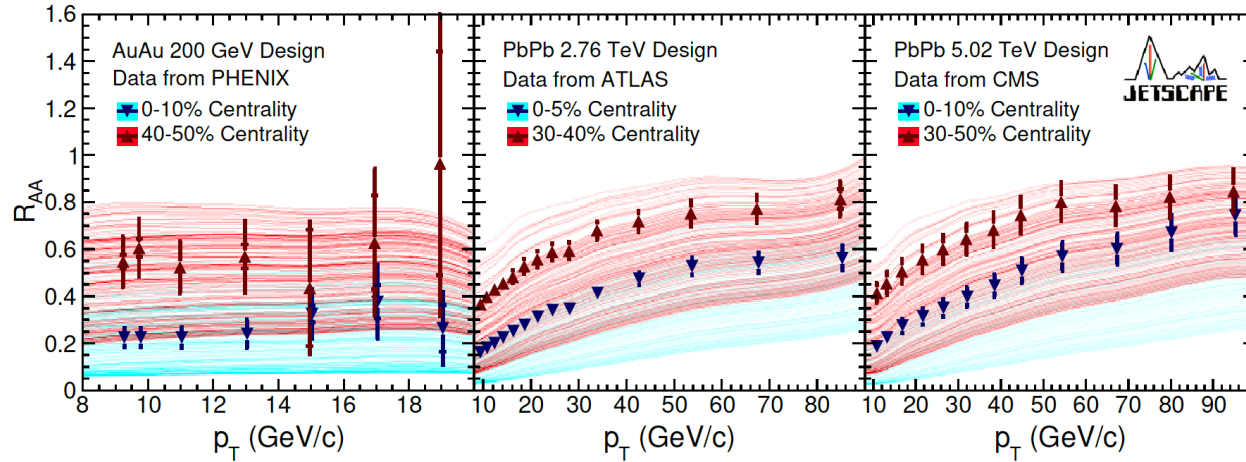


Consistent with JET results.

Only a **weak** temperature dependence of \hat{q}/T^3 is found.

Temperature dependence of \hat{q} from Bayesian analysis

JETSCAPE, PRC **104**, 024905 (2021)



Consistent with JET results.

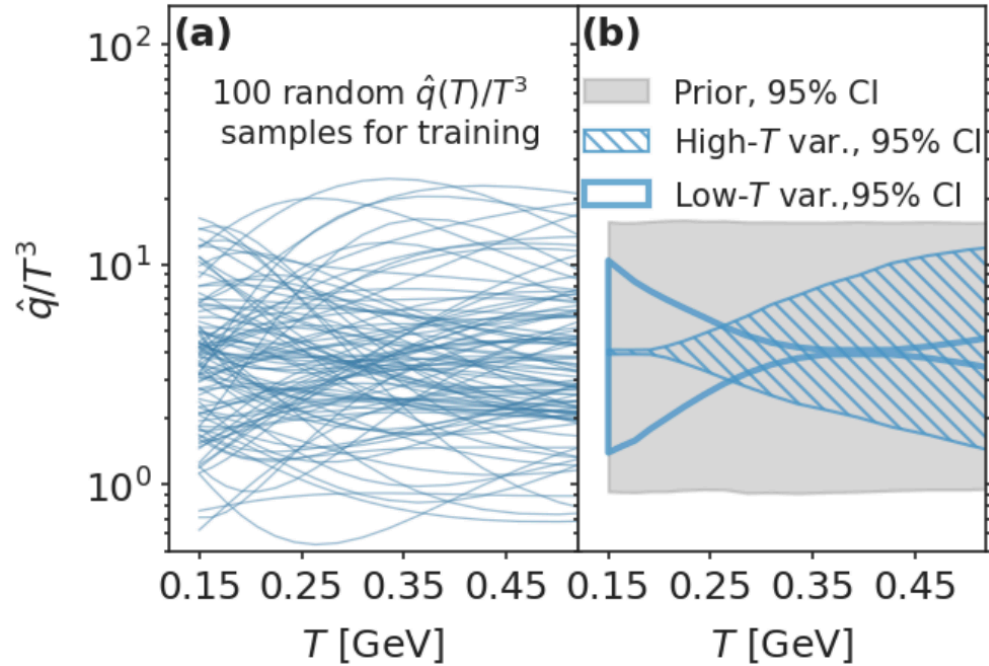
Only a **weak** temperature dependence of \hat{q}/T^3 is found.

$$\frac{\hat{q}(Q, E, T)|_{Q_0, A, C, D}}{T^3} = 42C_R \frac{\zeta(3)}{\pi} \left(\frac{4\pi}{9}\right)^2 \left\{ \frac{A[\ln(\frac{Q}{\Lambda}) - \ln(\frac{Q_0}{\Lambda})]}{[\ln(\frac{Q}{\Lambda})]^2} \theta(Q - Q_0) + \frac{C[\ln(\frac{E}{T}) - \ln(D)]}{[\ln(\frac{ET}{\Lambda^2})]^2} \right\}.$$

May be limited by parametrization form.

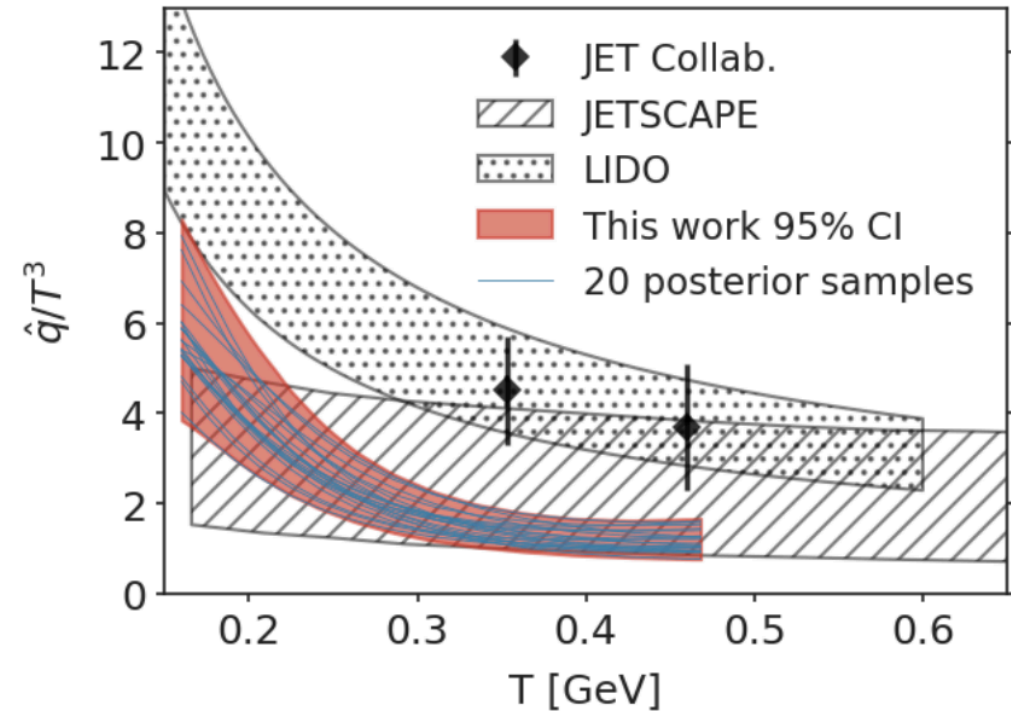
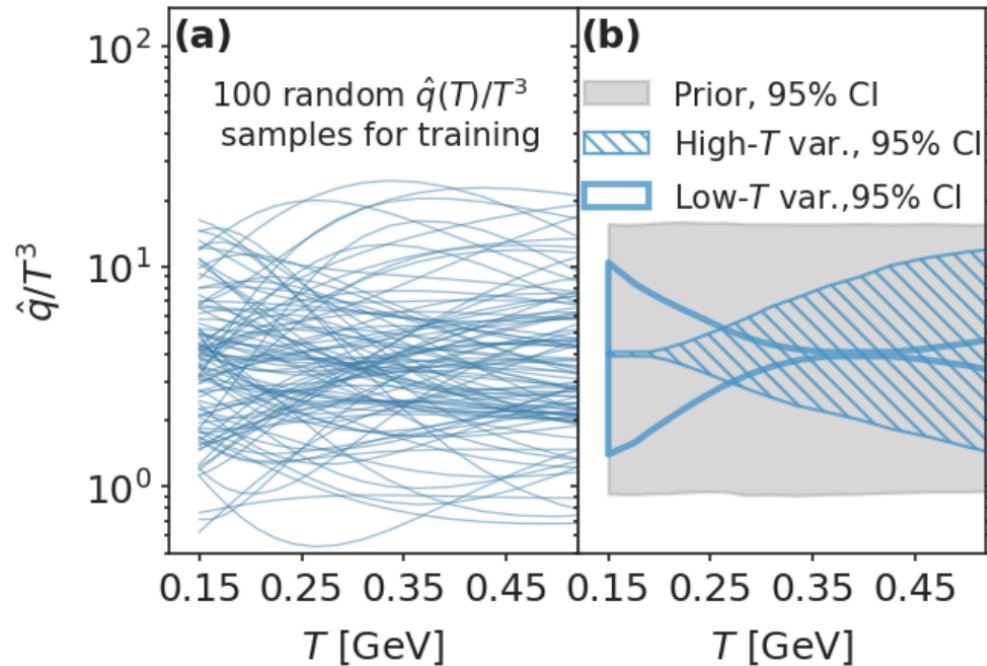
Temperature dependence of \hat{q} from Bayesian analysis

M. Xie, W. Ke, H. Zhang, X.-N. Wang, 2206.01340 [hep-ph]



Temperature dependence of \hat{q} from Bayesian analysis

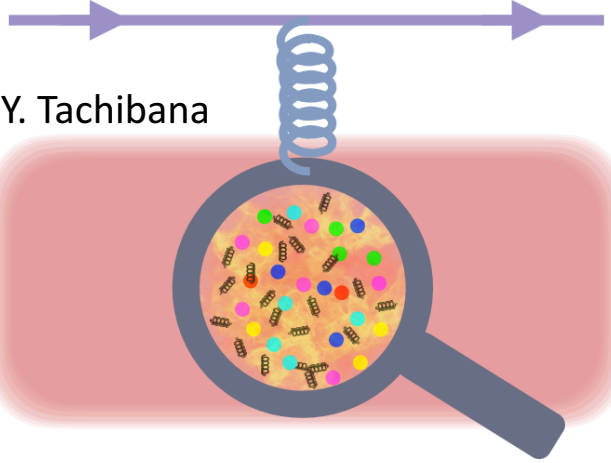
M. Xie, W. Ke, H. Zhang, X.-N. Wang, 2206.01340 [hep-ph]



A **strong** temperature dependence can be observed by introducing a parametrization-free information field method.

Dependence on kinematic variables

Jet Parton



From Y. Tachibana

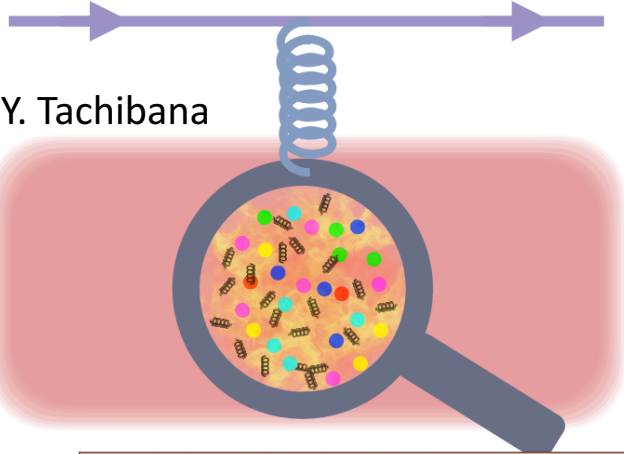
To decode more
microscopic fine
structures



Dependence of \hat{q} on
kinematic variables

Dependence on kinematic variables

Jet Parton



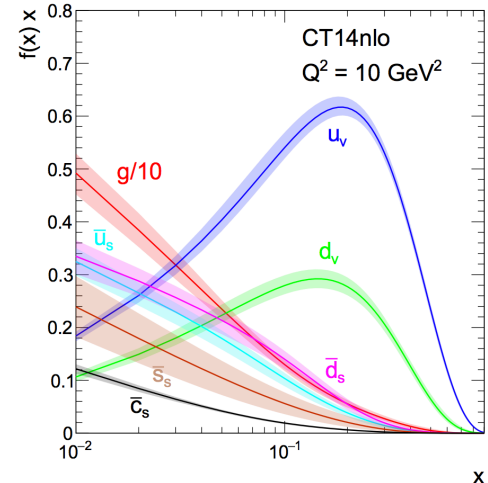
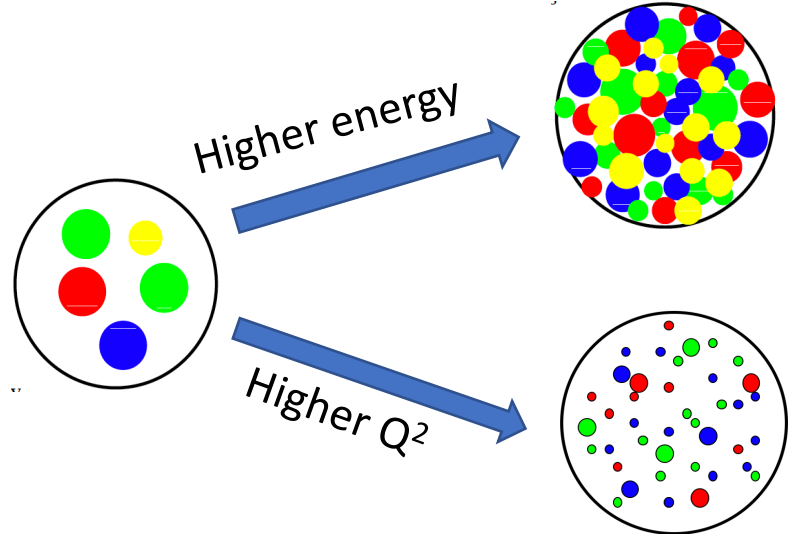
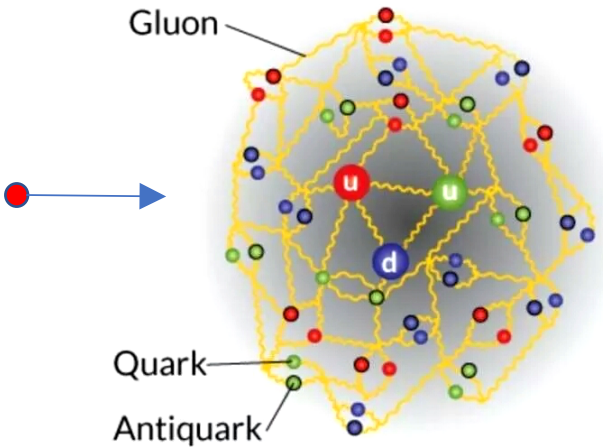
From Y. Tachibana

To decode more microscopic fine structures



Dependence of \hat{q} on kinematic variables

An analogy: Kinematic dependence of partonic structure of nucleon/nucleus:

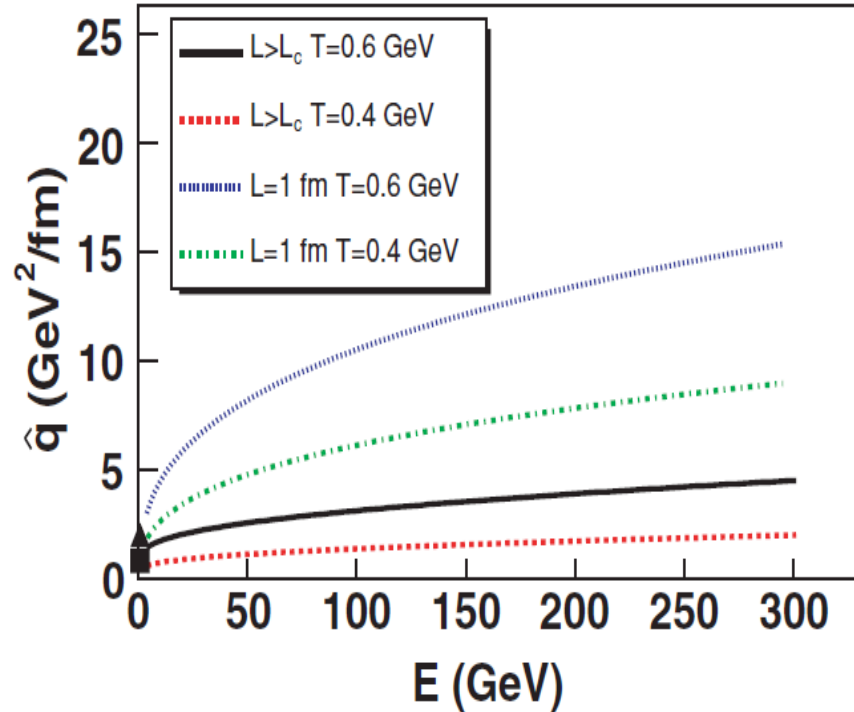


PDFs: global analysis based on factorization

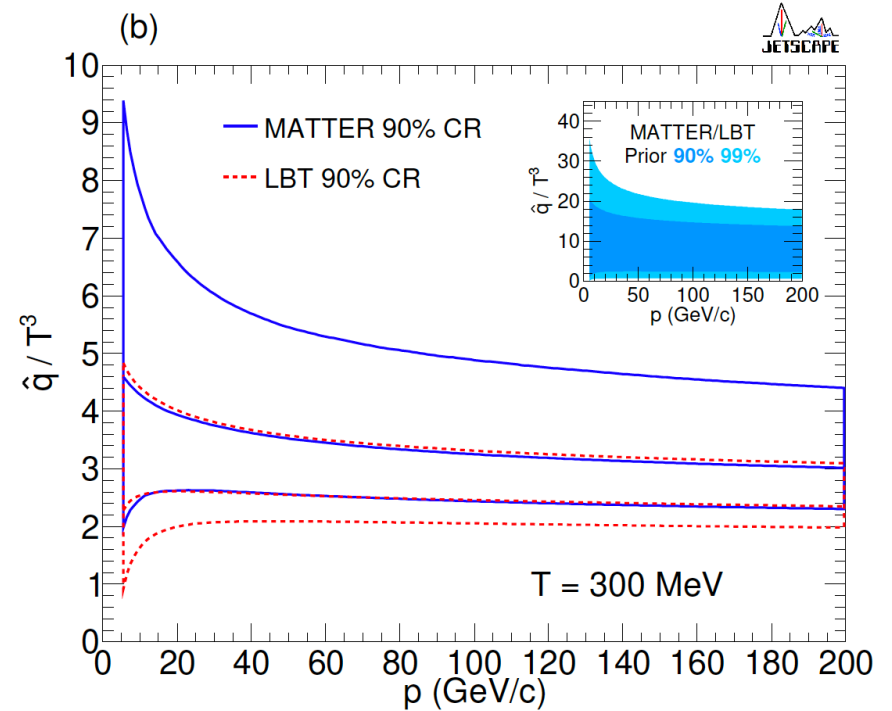


Dependence of \hat{q} on kinematic variables

J. Casalderrey-Solana and X.-N. Wang,
PRC 77, 024902 (2008)



JETSCAPE, PRC **104**, 024905 (2021)



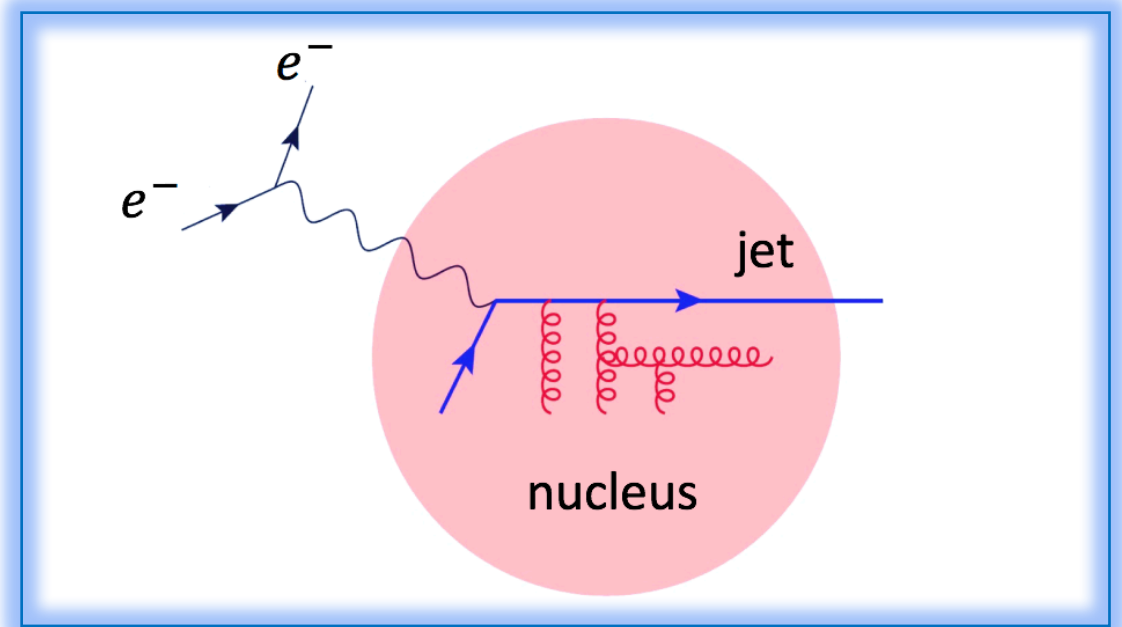
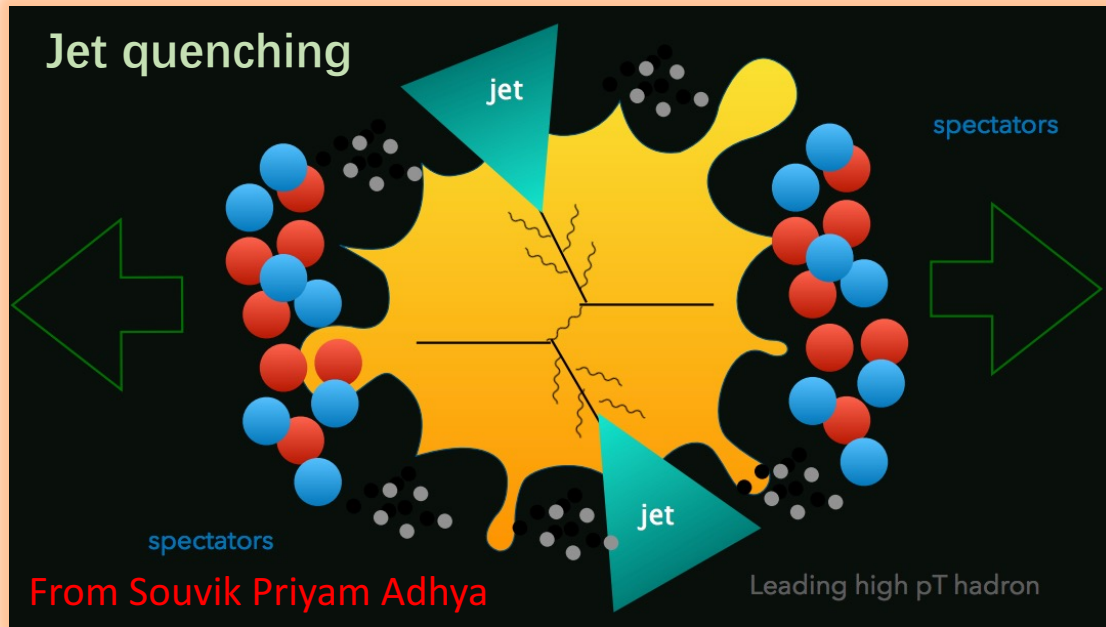
No clear energy dependence from Bayesian analysis.

1. Complicated system: uncertainties in both theoretical and experimental sides.

2. Limitation of the parametrization form.

3. Need more suitable observable to reveal such subtle kinematic dependence.

An ideal place to study kinematic dependence of \hat{q}



Advantages of eA/pA collisions:

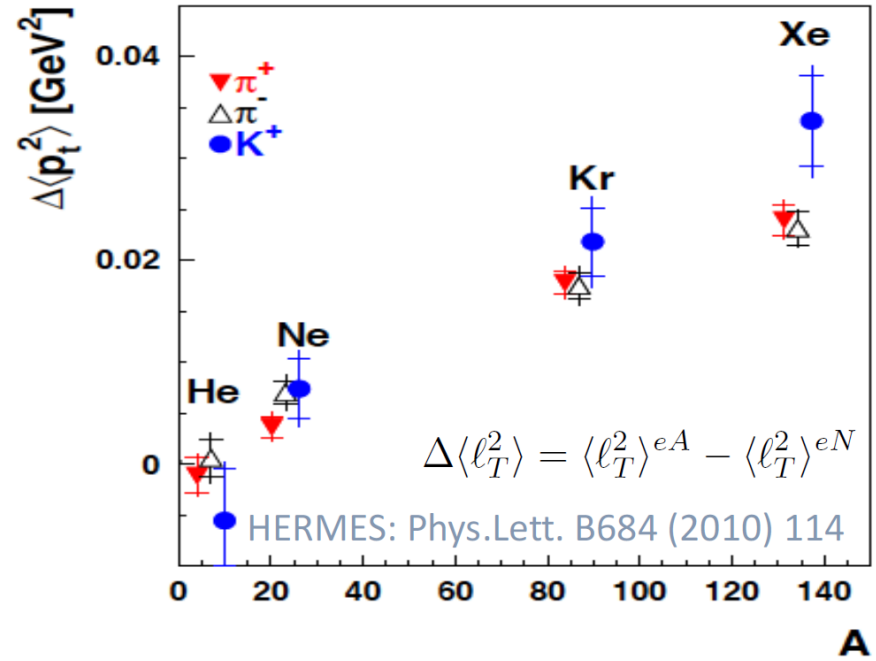
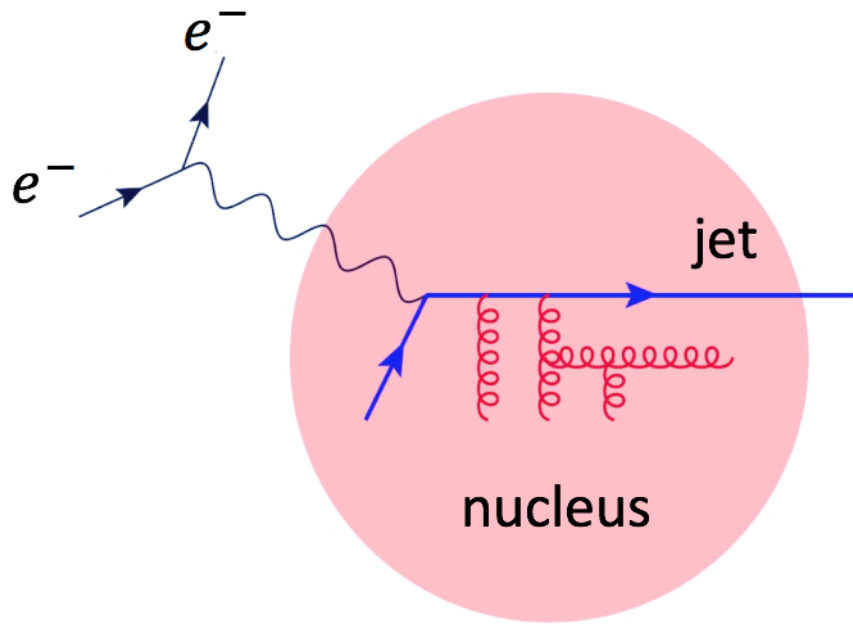
Less uncertainties in both theoretical and experimental sides.

More controllable kinematics.

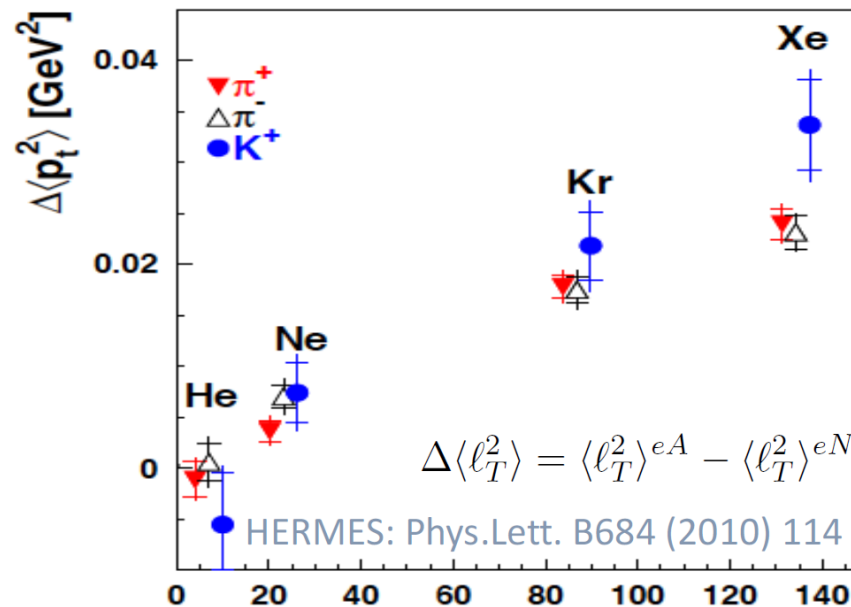
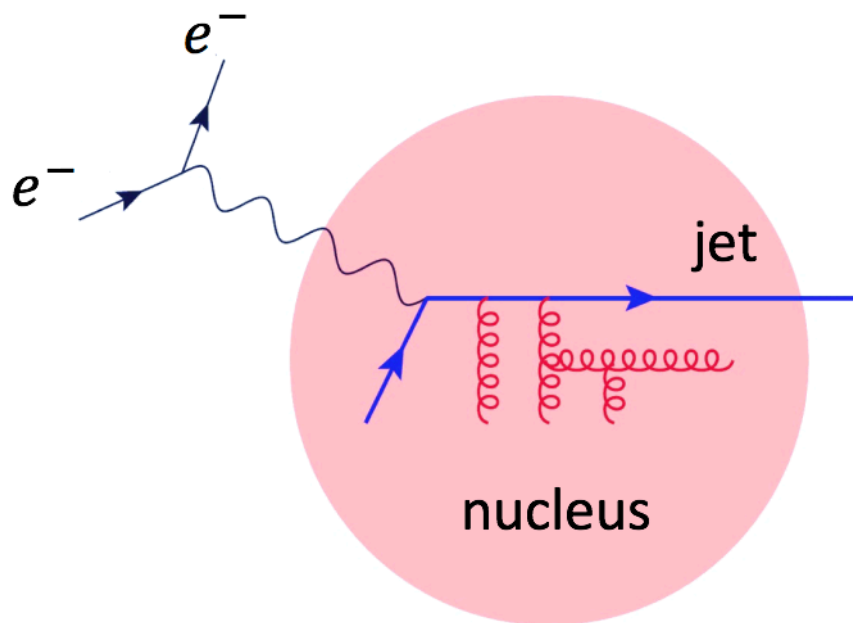
May be instructive for jet quenching in AA.

Opportunities from future high-precision EIC facilities.

\hat{q} and transverse momentum broadening



\hat{q} and transverse momentum broadening



Transverse momentum broadening: $\Delta\langle p_T^2 \rangle = \langle p_T^2 \rangle_{eA} - \langle p_T^2 \rangle_{ep}$

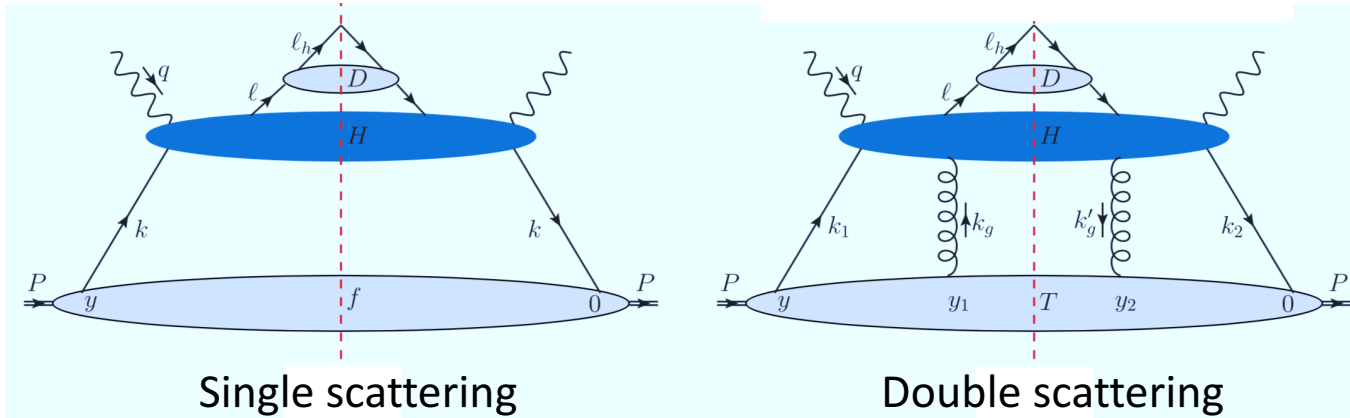
The nuclear-effect observable most directly related to \hat{q}

Increase with the mass number of the nuclear target

Multiple parton scattering in HT framework

Transverse momentum broadening in semi-inclusive deeply inelastic scattering (SIDIS)

$$d\sigma = d\sigma^S + d\sigma^D + \dots$$



Qiu & Sterman, NPB **353** (1991), **137** (1991).
Luo, Qiu, Sterman, PLB **279** (1992).

$$\sigma_{phys}^h = \begin{aligned} & \xrightarrow{\text{perturbative expansion}} \left[\alpha_s^0 C_2^{(0)} + \alpha_s^1 C_2^{(1)} + \alpha_s^2 C_2^{(2)} + \dots \right] \otimes T_2(x) \longrightarrow \text{leading twist} \\ & + \frac{1}{Q} \left[\alpha_s^0 C_3^{(0)} + \alpha_s^1 C_3^{(1)} + \alpha_s^2 C_3^{(2)} + \dots \right] \otimes T_3(x) \longrightarrow \text{twist-3} \\ & \xrightarrow{\text{power expansion}} \left[\frac{1}{Q^2} \left[\alpha_s^0 C_4^{(0)} + \alpha_s^1 C_4^{(1)} + \alpha_s^2 C_4^{(2)} + \dots \right] \otimes T_4(x) \longrightarrow \text{twist-4} \right. \\ & \left. + \dots \right] \end{aligned}$$

For SIDIS:

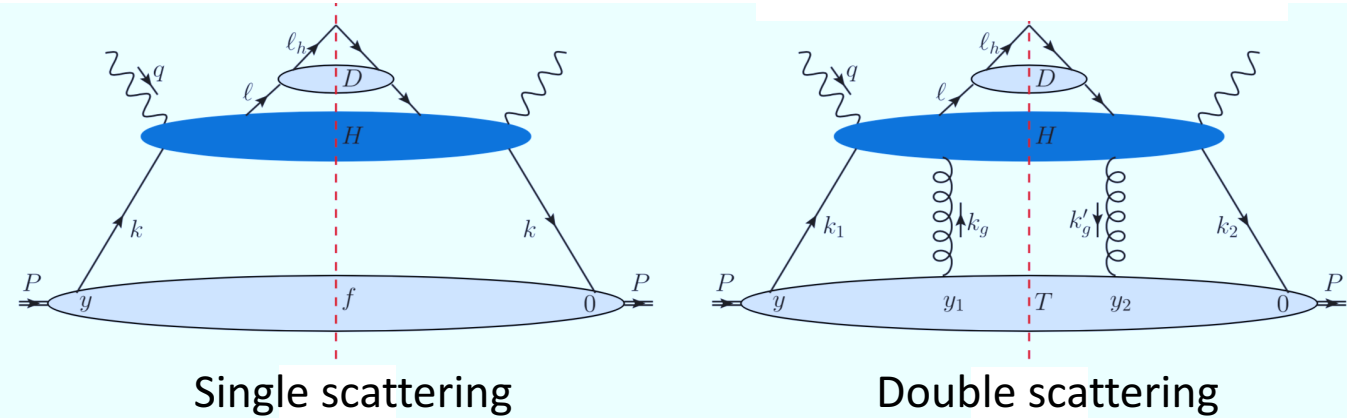
Guo, Phys. Rev. D **58**, 114033 (1998).

Kang, Wang, Wang, Xing, PRL **112**, 102001 (2014).

Multiple parton scattering in HT framework

Transverse momentum broadening in semi-inclusive deeply inelastic scattering (SIDIS)

$$d\sigma = d\sigma^S + d\sigma^D + \dots$$



Twist-4 quark-gluon correlation function:

$$T_{qg}(x) = \int \frac{dy^-}{2\pi} e^{ixp^+y^-} \int \frac{dy_1^- dy_2^-}{4\pi} \theta(-y_2^-) \theta(y^- - y_1^-) \langle p_A | F_{\alpha^+}(y_2^-) \bar{\Psi}_q(0) \gamma^+ \Psi_q(y^-) F^{\alpha^+}(y_1^-) | p_A \rangle$$

Transverse momentum broadening:

$$\Delta \langle p_T^2 \rangle \approx \int dp_T^2 p_T^2 \frac{d\sigma^D}{dPS dp_T^2} / \frac{d\sigma^S}{dPS} = \frac{8\pi^2 \alpha_s z_h^2 C_F}{N_c^2 - 1} \frac{\sum_q e_q^2 T_{qg}(x, \mu^2) D_{h/q}(z_h, \mu^2)}{\sum_q e_q^2 f_{q/A}(x, \mu^2) D_{h/q}(z_h, \mu^2)}$$

Qiu & Sterman, NPB 353 (1991), 137 (1991).
Luo, Qiu, Sterman, PLB 279 (1992).

$$\sigma_{phys}^h = \begin{aligned} & \xrightarrow{\text{perturbative expansion}} \left[\alpha_s^0 C_2^{(0)} + \alpha_s^1 C_2^{(1)} + \alpha_s^2 C_2^{(2)} + \dots \right] \otimes T_2(x) \longrightarrow \text{leading twist} \\ & + \frac{1}{Q} \left[\alpha_s^0 C_3^{(0)} + \alpha_s^1 C_3^{(1)} + \alpha_s^2 C_3^{(2)} + \dots \right] \otimes T_3(x) \longrightarrow \text{twist-3} \\ & \xrightarrow{\text{power expansion}} \left[\frac{1}{Q^2} \left[\alpha_s^0 C_4^{(0)} + \alpha_s^1 C_4^{(1)} + \alpha_s^2 C_4^{(2)} + \dots \right] \otimes T_4(x) \longrightarrow \text{twist-4} \right. \\ & \left. + \dots \right] \end{aligned}$$

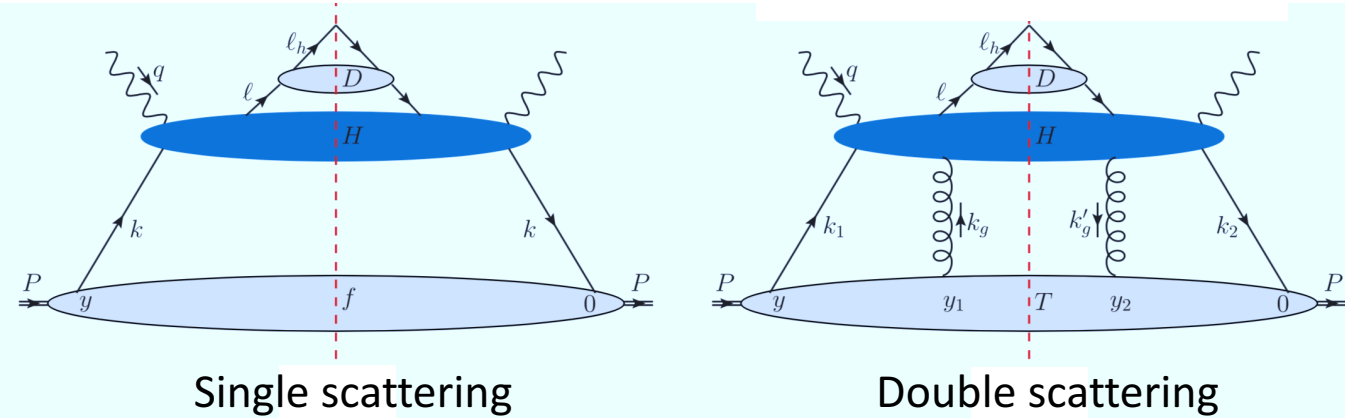
For SIDIS:
Guo, Phys. Rev. D 58, 114033 (1998).
Kang, Wang, Wang, Xing, PRL 112, 102001 (2014).



Multiple parton scattering in HT framework

Transverse momentum broadening in semi-inclusive deeply inelastic scattering (SIDIS)

$$d\sigma = d\sigma^S + d\sigma^D + \dots$$



Twist-4 quark-gluon correlation function:

$$T_{qg}(x) = \int \frac{dy^-}{2\pi} e^{ixp^+y^-} \int \frac{dy_1^- dy_2^-}{4\pi} \theta(-y_2^-) \theta(y^- - y_1^-) \langle p_A | F_{\alpha^+}^+(y_2^-) \bar{\Psi}_q(0) \gamma^+ \Psi_q(y^-) F^{\alpha^+}(y_1^-) | p_A \rangle$$

Transverse momentum broadening:

$$\Delta \langle p_T^2 \rangle \approx \int dp_T^2 p_T^2 \frac{d\sigma^D}{dPS dp_T^2} / \frac{d\sigma^S}{dPS} = \frac{8\pi^2 \alpha_s z_h^2 C_F}{N_c^2 - 1} \frac{\sum_q e_q^2 T_{qg}(x, \mu^2) D_{h/q}(z_h, \mu^2)}{\sum_q e_q^2 f_{q/A}(x, \mu^2) D_{h/q}(z_h, \mu^2)}$$

Expressed with \hat{q} :

$$T_{qg}(x, Q^2) \approx \frac{9R_A}{8\pi^2 \alpha_s} f_{q/A}(x, Q^2) \hat{q}(x, Q^2)$$

Approximation of a large and loosely bound nucleus

Qiu & Sterman, NPB **353** (1991), **137** (1991).
Luo, Qiu, Sterman, PLB **279** (1992).

$$\sigma_{phys}^h = \begin{aligned} & \xrightarrow{\text{perturbative expansion}} \left[\alpha_s^0 C_2^{(0)} + \alpha_s^1 C_2^{(1)} + \alpha_s^2 C_2^{(2)} + \dots \right] \otimes T_2(x) \longrightarrow \text{leading twist} \\ & + \frac{1}{Q} \left[\alpha_s^0 C_3^{(0)} + \alpha_s^1 C_3^{(1)} + \alpha_s^2 C_3^{(2)} + \dots \right] \otimes T_3(x) \longrightarrow \text{twist-3} \\ & \xrightarrow{\text{power expansion}} \left[\frac{1}{Q^2} \left[\alpha_s^0 C_4^{(0)} + \alpha_s^1 C_4^{(1)} + \alpha_s^2 C_4^{(2)} + \dots \right] \otimes T_4(x) \right] \longrightarrow \text{twist-4} \\ & + \dots \end{aligned}$$

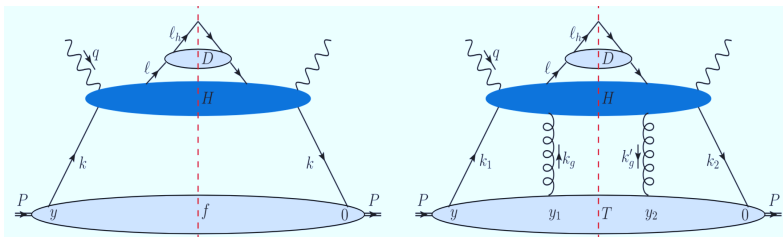
For SIDIS:

Guo, Phys. Rev. D **58**, 114033 (1998).

Kang, Wang, Wang, Xing, PRL **112**, 102001 (2014).

Multiple parton scattering in HT framework

1. SIDIS

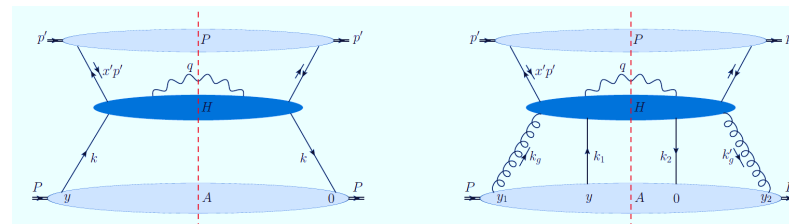


Single scattering

Double scattering

Guo (1998), Kang, et al.,(2014).

2. Drell-Yan (pA)



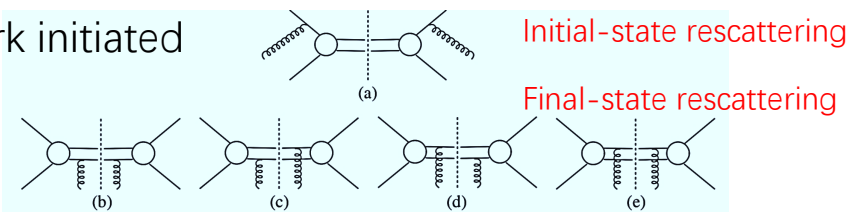
Single scattering

Double scattering

Kang & Qiu, PRD 77, 114027 (2008).

3. Heavy quarkonium (pA)

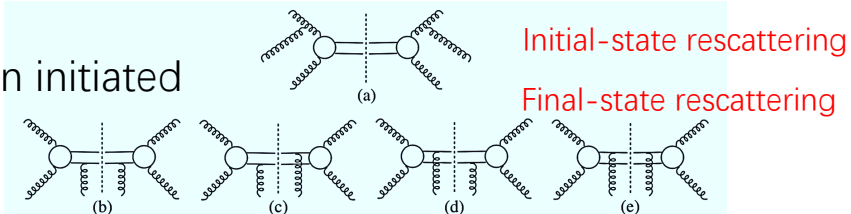
Quark initiated



Initial-state rescattering

Final-state rescattering

Gluon initiated

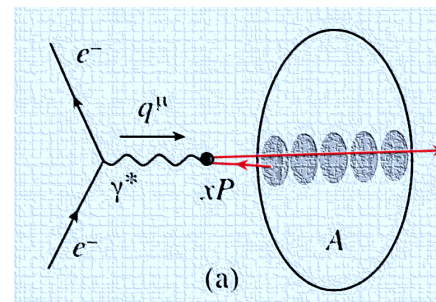


Initial-state rescattering

Final-state rescattering

Kang & Qiu, PRD 77, 114027 (2008), PLB 721, 277 (2013).

4. Dynamical shadowing. (DIS)

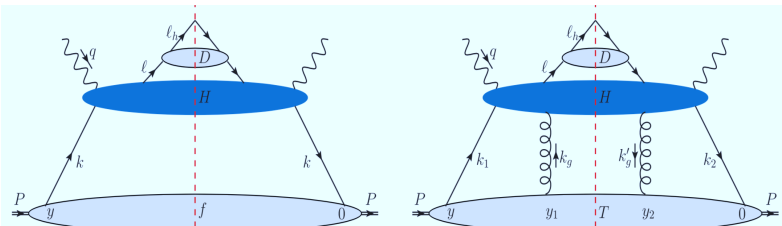


$$R(x, Q^2) = \frac{F_2^A(x, Q^2)}{F_2^D(x, Q^2)}$$

Qiu & Vitev, PRL 93, 262301 (2004).

Multiple parton scattering in HT framework

1. SIDIS

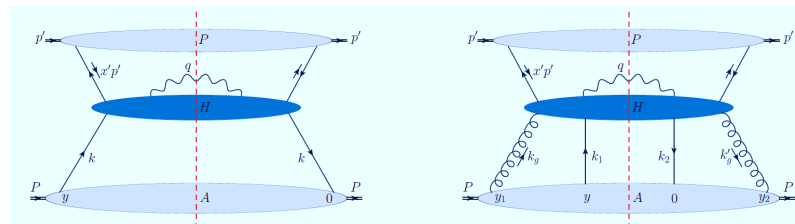


Single scattering

Double scattering

Guo (1998), Kang, et al., (2008)

2. Drell-Yan (pA)



Single scattering

Double scattering

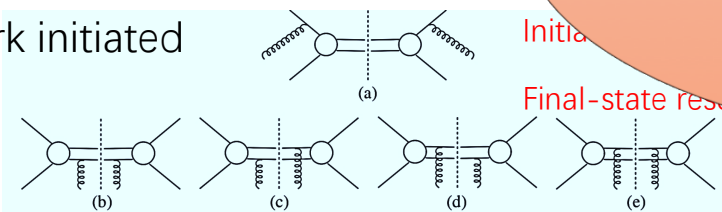
Qiu & Vitev, PRD 77, 114027 (2008).

A Common parameter:

\hat{q} in CNM

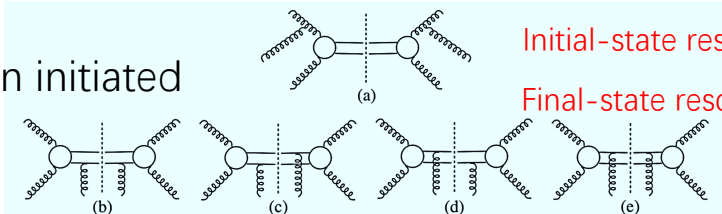
3. Heavy quarkonia

Quark initiated



Initial-state rescattering
Final-state rescattering

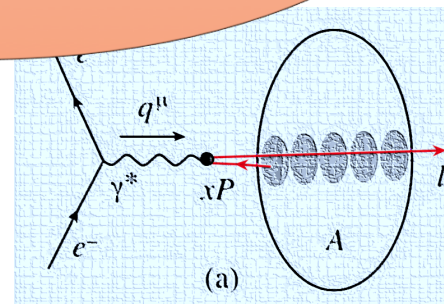
Gluon initiated



Initial-state rescattering
Final-state rescattering

Kang & Qiu, PRD 77, 114027 (2008), PLB 721, 277 (2013).

Final state shadowing.
(DIS)

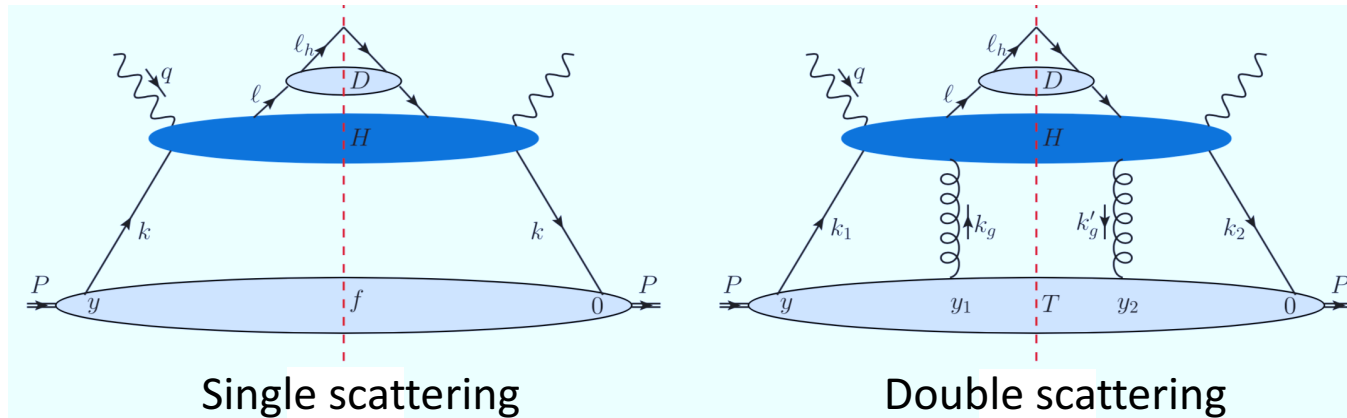


$$R(x, Q^2) = \frac{F_2^A(x, Q^2)}{F_2^D(x, Q^2)}$$

Qiu & Vitev, PRL 93, 262301 (2004).

Multiple parton scattering in HT framework

Generalizing co-linear factorization to multiple scattering (higher twist)



Single scattering

Double scattering

Parton distribution function

$$f_q(x, Q^2)$$



$$T_{qg}(x, Q^2)$$

Quark-gluon correlation function

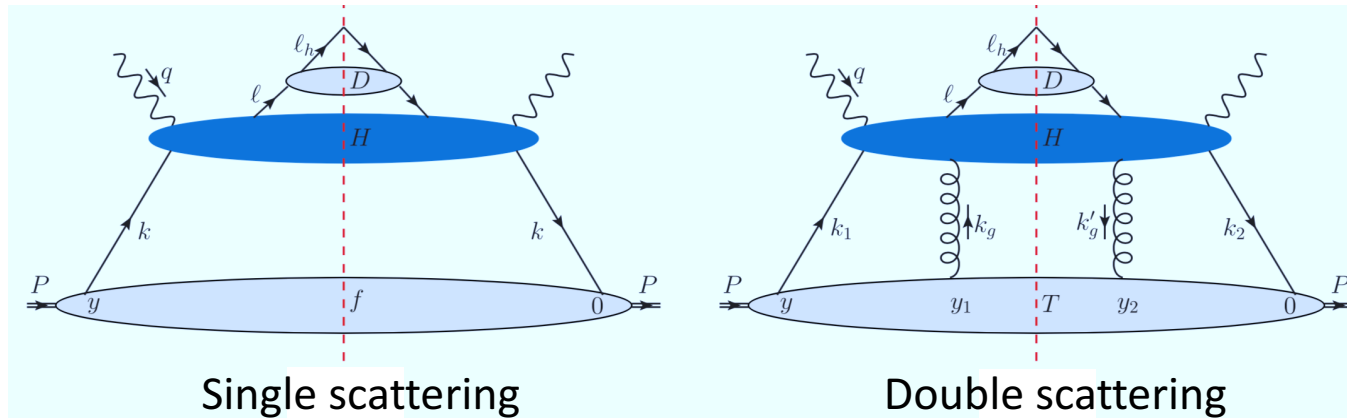
HT factorization verified to NLO

LO: Guo, Phys. Rev. D 58, 114033 (1998).

NLO: Kang, Wang, Wang, Xing, PRL 112, 102001 (2014).

Multiple parton scattering in HT framework

Generalizing co-linear factorization to multiple scattering (higher twist)



Single scattering

Double scattering

Parton distribution function

$$f_q(x, Q^2)$$



$$T_{qg}(x, Q^2)$$

Quark-gluon correlation function

HT factorization verified to NLO

LO: Guo, Phys. Rev. D 58, 114033 (1998).

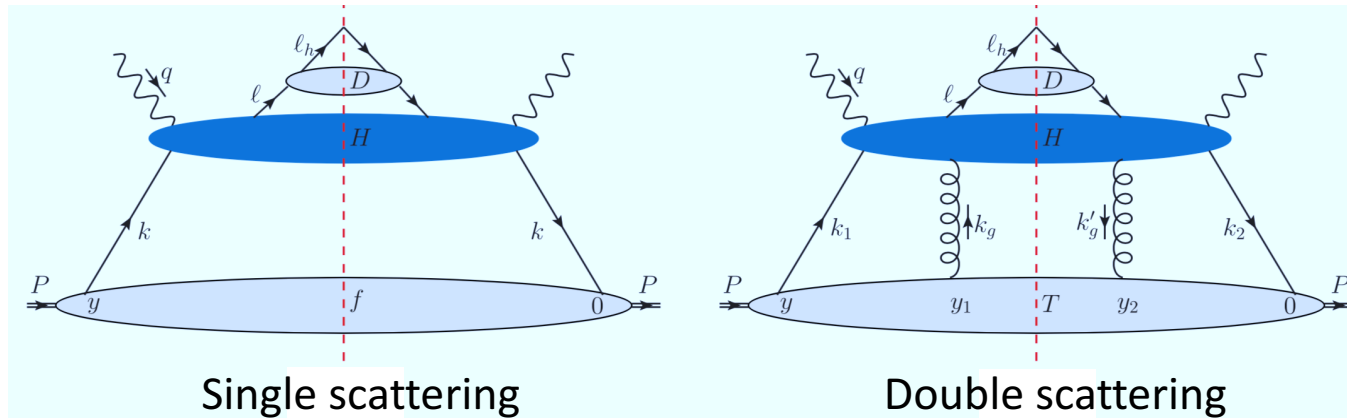
NLO: Kang, Wang, Wang, Xing, PRL 112, 102001 (2014).

$$\hat{q}(x, Q^2) \approx \frac{8\pi^2 \alpha_s}{9R_A} \frac{T_{qg}(x, Q^2)}{f_{q/A}(x, Q^2)}$$

Dependence on Kinematic variables (x, Q^2) is naturally included.

Multiple parton scattering in HT framework

Generalizing co-linear factorization to multiple scattering (higher twist)



Measurement of $\Delta\langle p_T^2 \rangle$
at certain values of
Bjorken x_B and scale Q^2

$$\hat{q}(x_B, Q^2)$$

Parton distribution function

$$f_q(x, Q^2)$$



$$T_{qg}(x, Q^2)$$

Quark-gluon correlation function

HT factorization verified to NLO

LO: Guo, Phys. Rev. D 58, 114033 (1998).

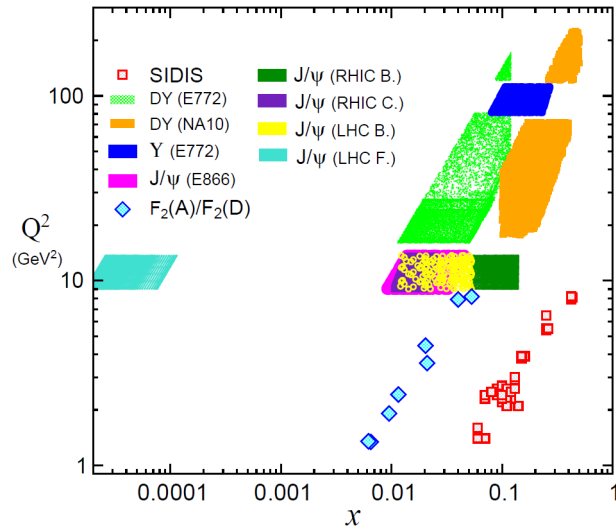
NLO: Kang, Wang, Wang, Xing, PRL 112, 102001 (2014).

$$\hat{q}(x, Q^2) \approx \frac{8\pi^2 \alpha_s}{9R_A} \frac{T_{qg}(x, Q^2)}{f_{q/A}(x, Q^2)}$$

Dependence on Kinematic variables (x, Q^2)
is naturally included.

Extract \hat{q} & study its kinematic dependence

Range of kinematics (x and Q^2) covered by chosen data:



PR, Z.B. Kang, E. Wang, H. Xing and B.W. Zhang, PRD, L031901 (2021).

Parametrization of $\hat{q}(x, Q^2)$:

$$\hat{q}(x, Q^2) = \hat{q}_0 \alpha_s(Q^2) x^\alpha (1-x)^\beta [\ln(Q^2/Q_0^2)]^\gamma$$

4 parameters to be constrained by data:

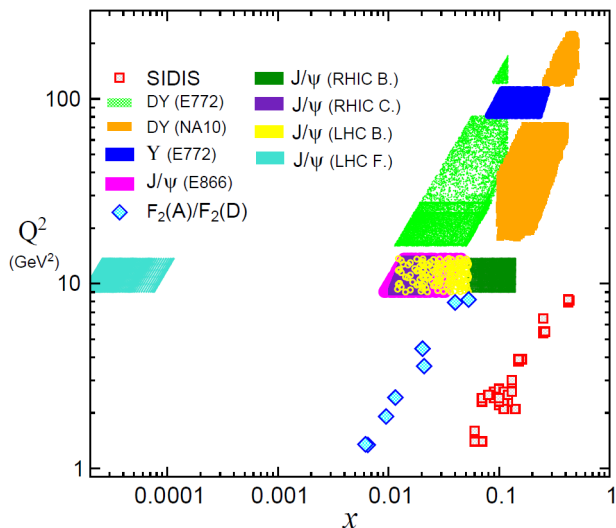
$$\hat{q}_0, \alpha, \beta, \gamma$$

Also test constant

$$\hat{q} = \hat{q}_0:$$

Extract \hat{q} & study its kinematic dependence

Range of kinematics (x and Q^2) covered by chosen data:



PR, Z.B. Kang, E. Wang, H. Xing and B.W. Zhang, PRD, L031901 (2021).

Parametrization of $\hat{q}(x, Q^2)$:

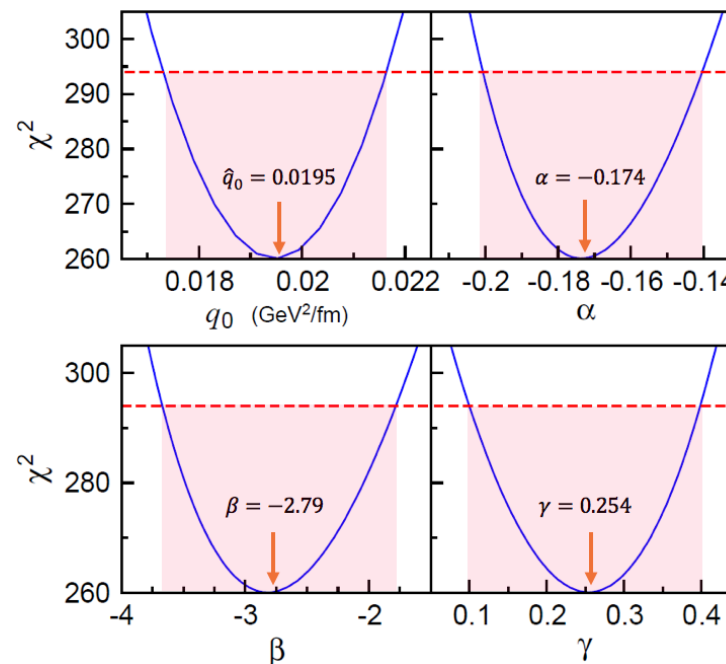
$$\hat{q}(x, Q^2) = \hat{q}_0 \alpha_s(Q^2) x^\alpha (1-x)^\beta [\ln(Q^2/Q_0^2)]^\gamma$$

4 parameters to be constrained by data:

$$\hat{q}_0, \alpha, \beta, \gamma$$

Also test constant

$$\hat{q} = \hat{q}_0:$$



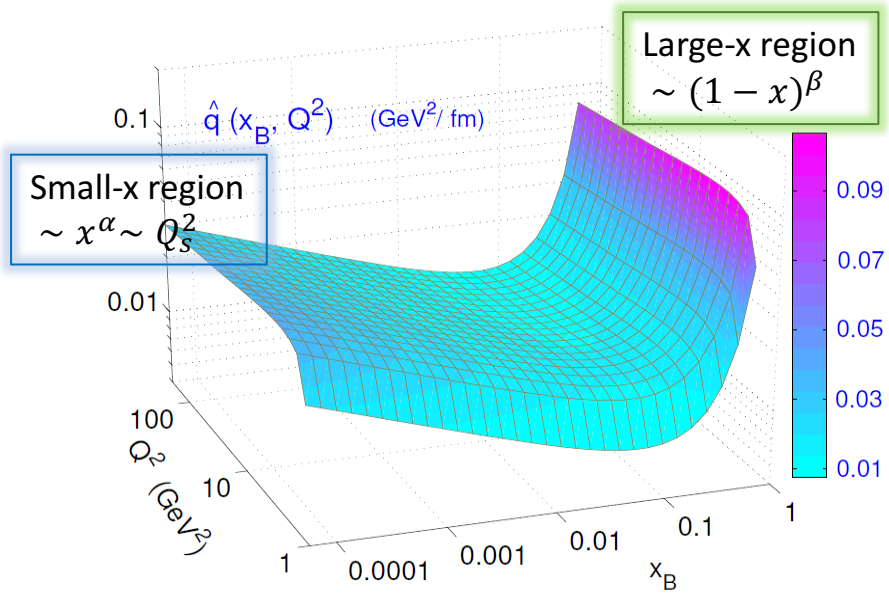
experiment	data type	data points	χ^2 (constant \hat{q})	χ^2 [$\hat{q}(x_B, Q^2)$]
HERMES	SIDIS (p_T broad.)	156	218.5	189.7
FNAL-E772	DY (p_T broad.)	4	2.69	1.65
SPS-NA10	DY (p_T broad.)	5	6.86	6.47
FNAL-E772	Υ (p_T broad.)	4	2.33	2.67
FNAL-E866	J/ψ (p_T broad.)	4	2.03	2.45
RHIC	J/ψ (p_T broad.)	10	44.4	31.0
LHC	J/ψ (p_T broad.)	12	87.3	4.8
FNAL-E665	DIS (shadowing)	20	23.7	21.46
TOTAL:		215	387.9	260.2

Table 1. Data sets used in the global analysis, and the χ^2 values with a constant \hat{q} and $\hat{q}(x_B, Q^2)$, respectively.

Extract \hat{q} & study its kinematic dependence

Optimal $\hat{q}(x, Q^2)$

$$\hat{q}(x, Q^2) = \hat{q}_0 \alpha_s(Q^2) x^\alpha (1-x)^\beta [\ln(Q^2/Q_0^2)]^\gamma$$

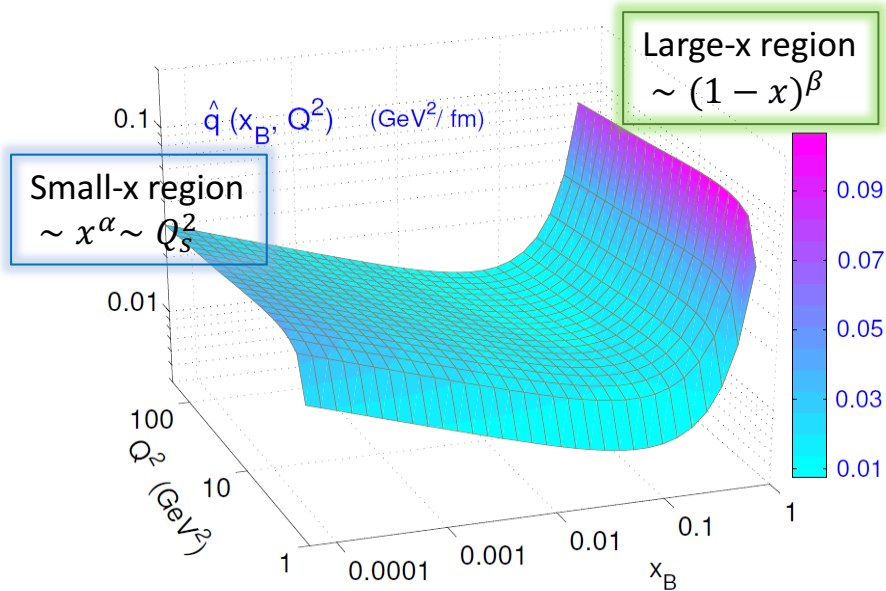


$$\hat{q}_0 = 0.0191 \pm 0.0061 \text{ GeV}^2/\text{fm}, \quad \alpha = -0.182 \pm 0.050$$
$$\beta = -2.85 \pm 1.87, \quad \gamma = 0.264 \pm 0.169.$$

Extract \hat{q} & study its kinematic dependence

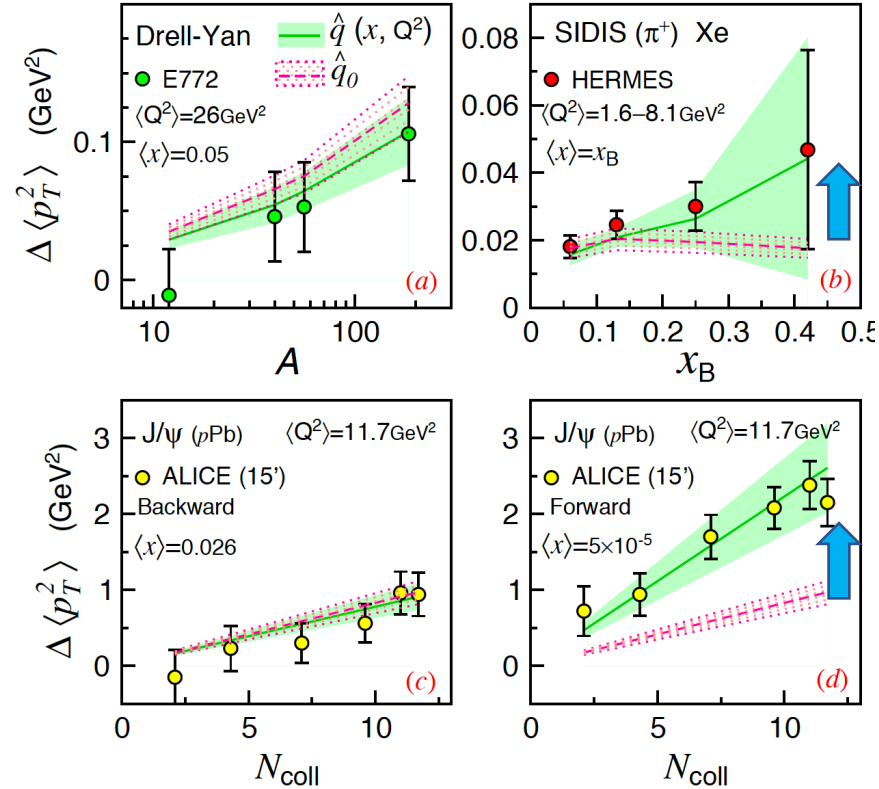
Optimal $\hat{q}(x, Q^2)$

$$\hat{q}(x, Q^2) = \hat{q}_0 \alpha_s(Q^2) x^\alpha (1-x)^\beta [\ln(Q^2/Q_0^2)]^\gamma$$



$$\hat{q}_0 = 0.0191 \pm 0.0061 \text{ GeV}^2/\text{fm}, \quad \alpha = -0.182 \pm 0.050$$

$$\beta = -2.85 \pm 1.87, \quad \gamma = 0.264 \pm 0.169.$$

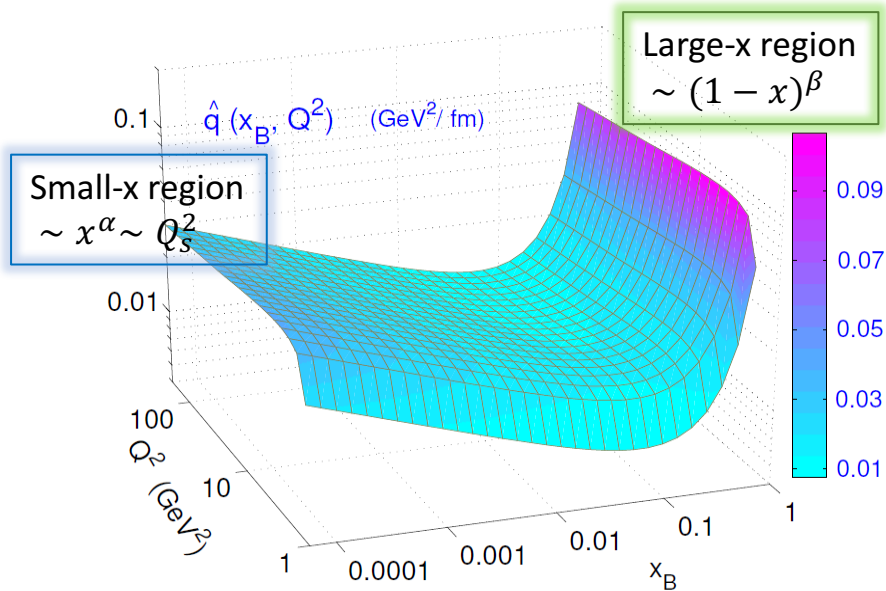


SIDIS in large-x region and
J/psi in forward (small-x) region
favor the enhanced broadening.

Extract \hat{q} & study its kinematic dependence

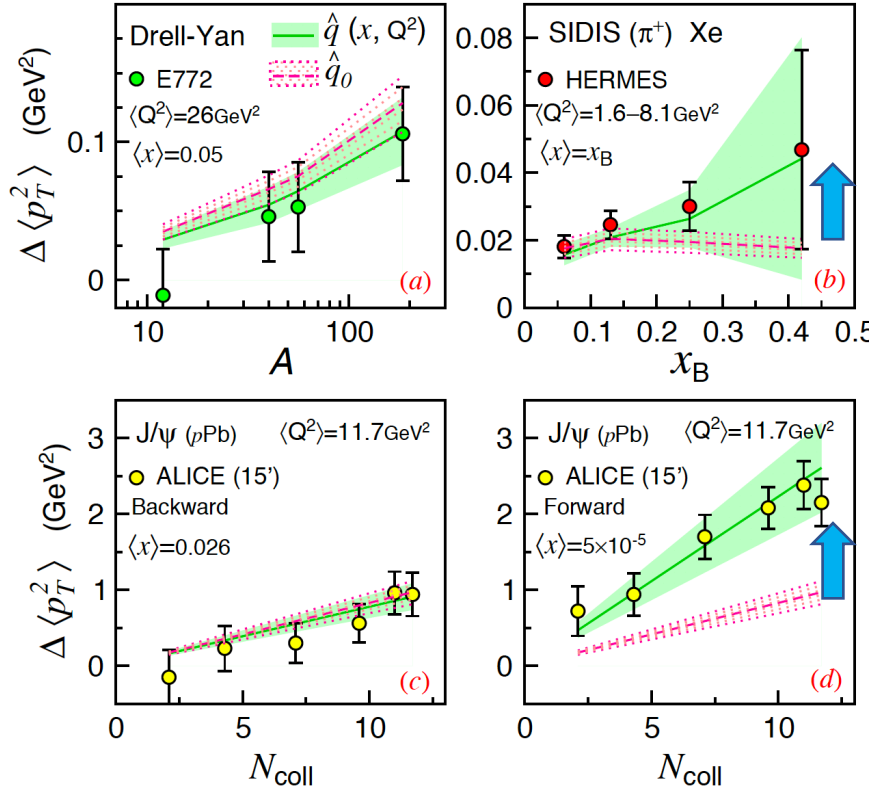
Optimal $\hat{q}(x, Q^2)$

$$\hat{q}(x, Q^2) = \hat{q}_0 \alpha_s(Q^2) x^\alpha (1-x)^\beta [\ln(Q^2/Q_0^2)]^\gamma$$



$$\hat{q}_0 = 0.0191 \pm 0.0061 \text{ GeV}^2/\text{fm}, \quad \alpha = -0.182 \pm 0.050$$

$$\beta = -2.85 \pm 1.87, \quad \gamma = 0.264 \pm 0.169.$$



SIDIS in large-x region and J/psi in forward (small-x) region favor the enhanced broadening.

Seems consistent with recent study.

Arleo and Naim, JHEP (2021)
Extraction from DY and quarkonium data:

$$\hat{q}_A(x) = \hat{q}_0 \times \left(\frac{10^{-2}}{x}\right)^\alpha \quad \hat{q}_0 = 0.051 \sim 0.075$$

$$\alpha = 0.25 - 0.3$$

Y.-Y. Zhang, X.-N. Wang,
PRD 105 034015 (2022)

$$\hat{q}_A^0(x_B, Q^2) = \frac{A^{1/3}}{2R_A} Q_{s0}^2(x_B, Q^2).$$

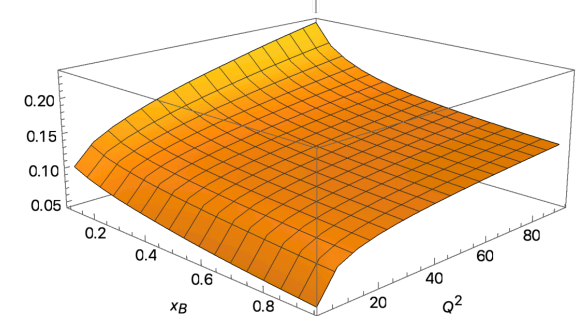
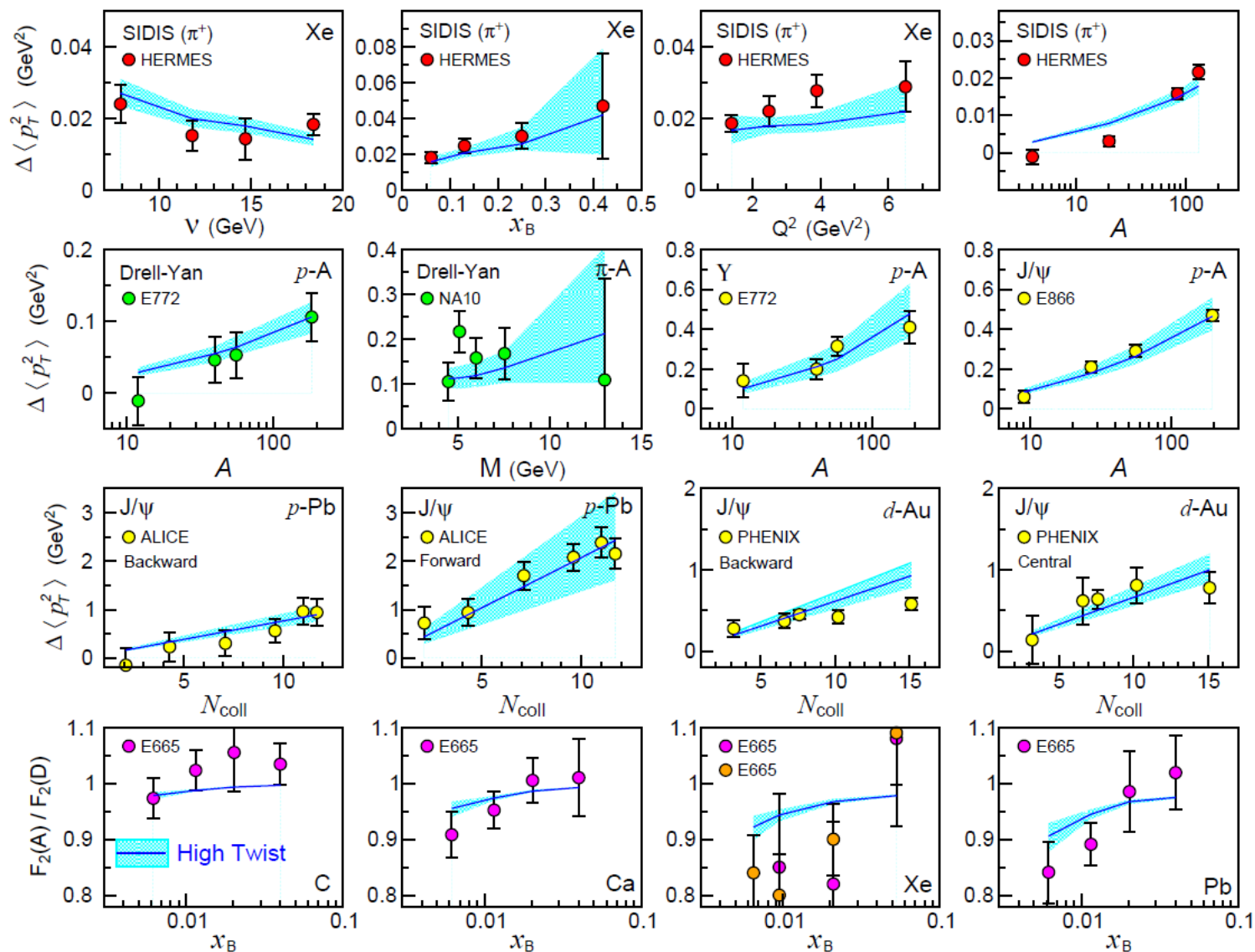
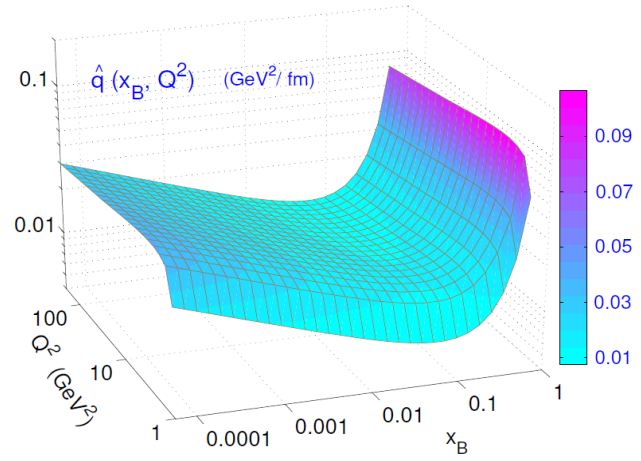


FIG. 5. The x_B and Q^2 dependence of the scaled saturation scale $Q_{s0}^2(x_B, Q^2)$ inside Pb from solving Eq. (29).

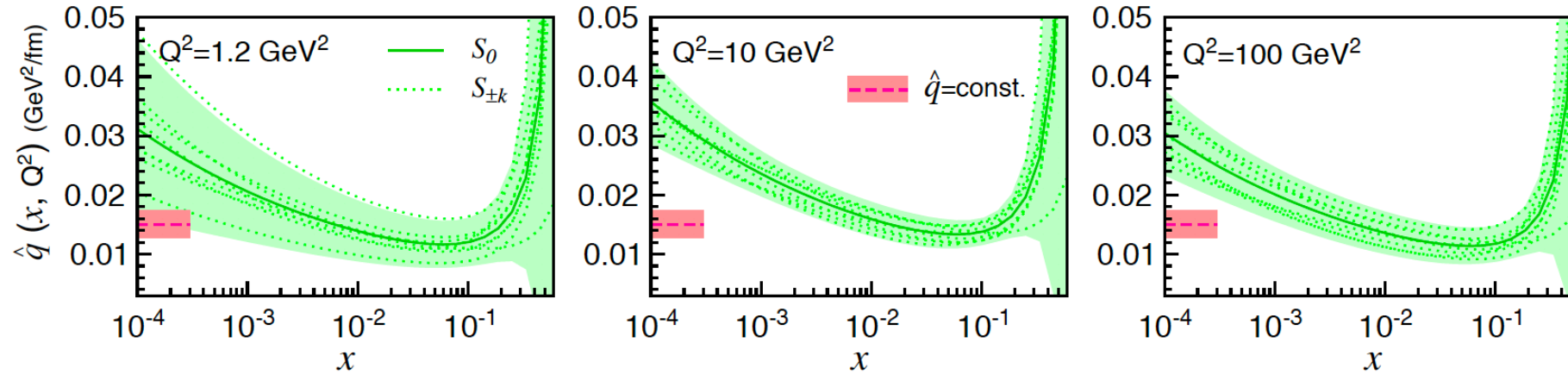
HT results with extracted $\hat{q}(x, Q^2)$



Determine uncertainties of \hat{q}

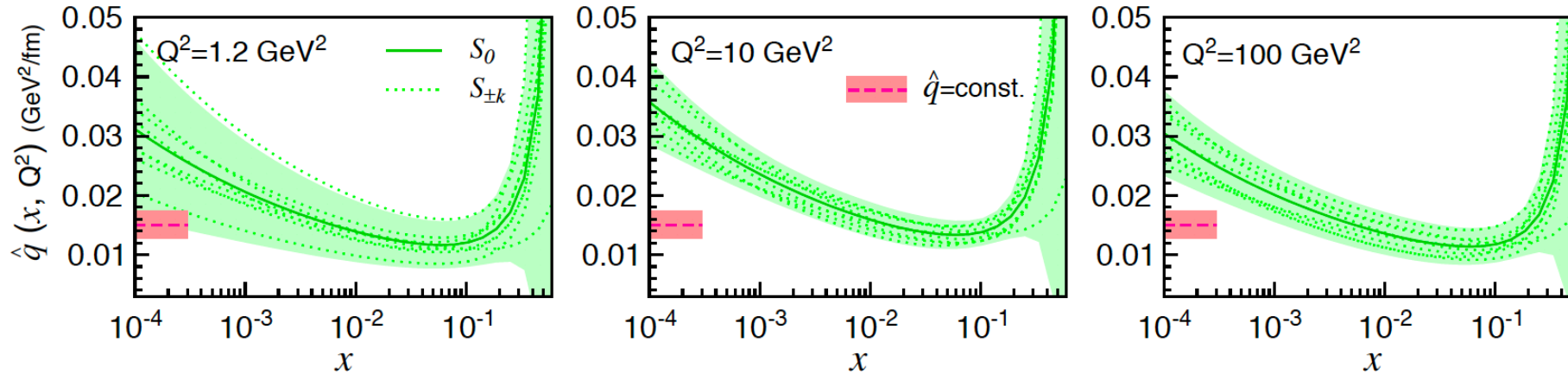


Determine uncertainties of \hat{q}



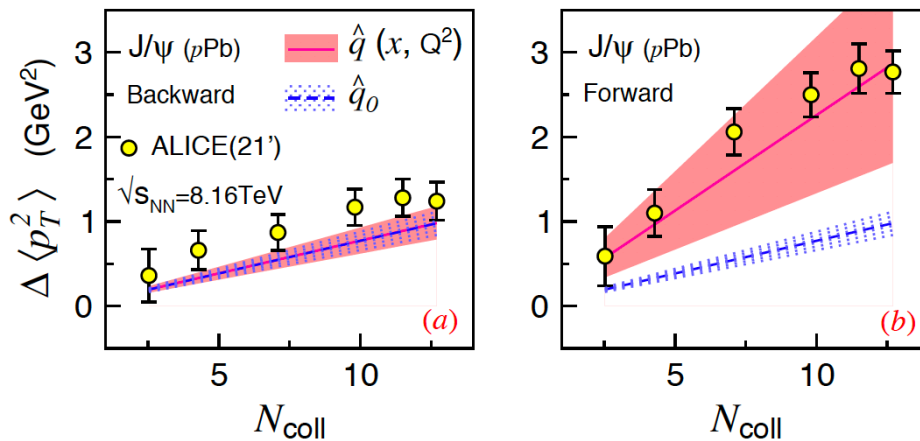
Hessian matrix method [PRD,65,014011, widely used in the analysis of PDFs, to determine the uncertainty of \hat{q} in cold nuclear matter. **Nine sets** S_k ($k=-4, \dots, 0, \dots, 4$) of $\hat{q}(x, Q^2)$ for future theoretical predictions.

Determine uncertainties of \hat{q}

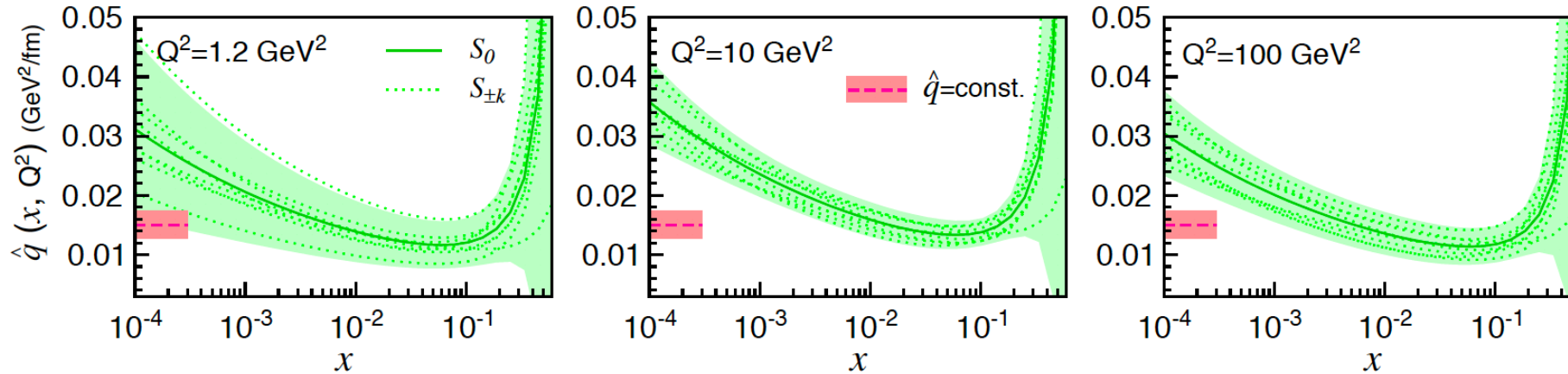


Hessian matrix method [PRD,65,014011, widely used in the analysis of PDFs, to determine the uncertainty of \hat{q} in cold nuclear matter. **Nine sets** $S_k, (k=-4, \dots, 0, \dots, 4)$ of $\hat{q}(x, Q^2)$ for future theoretical predictions.

Test with new LHC data on Jpsi

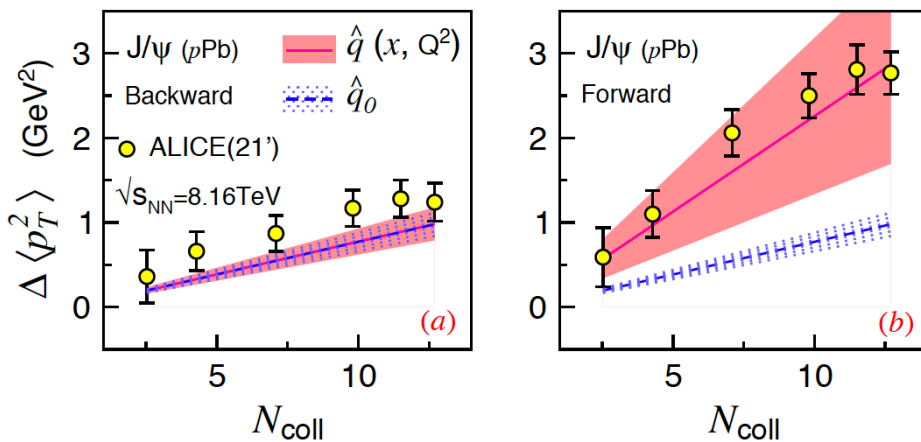


Determine uncertainties of \hat{q}

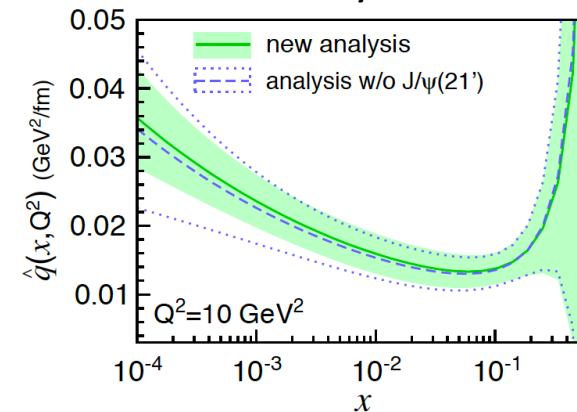


Hessian matrix method [PRD,65,014011, widely used in the analysis of PDFs, to determine the uncertainty of \hat{q} in cold nuclear matter. **Nine sets** $S_k, (k=-4, \dots, 0, \dots, 4)$ of $\hat{q}(x, Q^2)$ for future theoretical predictions.

Test with new LHC data on Jpsi

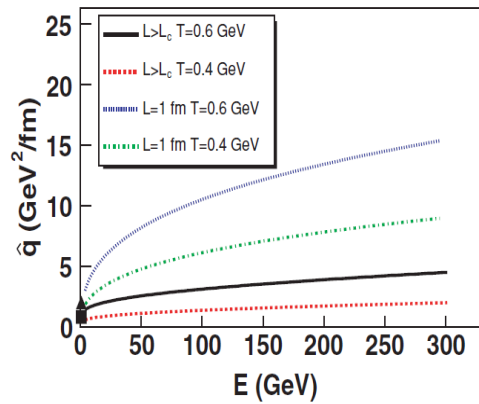


New data reduce uncertainty at small x

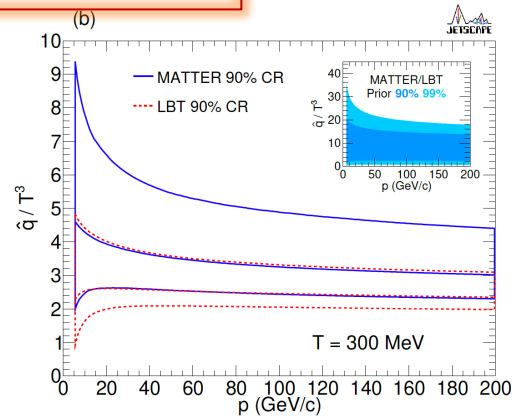


\hat{q} for cold nuclear matter: jet energy dependence

For quark-gluon plasma



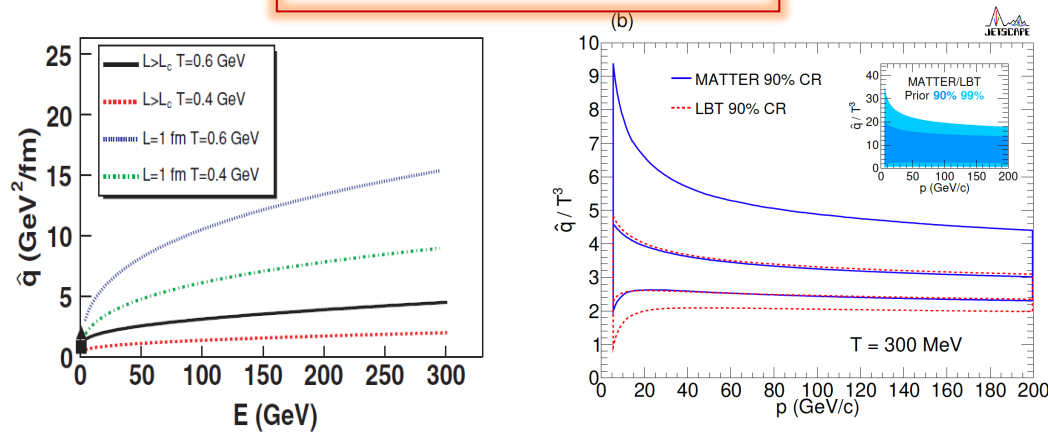
J. Casalderrey-Solana and X.-N. Wang,
PRC **77**, 024902 (2008)



JETSCAPE, PRC **104**,
024905 (2021)

\hat{q} for cold nuclear matter: jet energy dependence

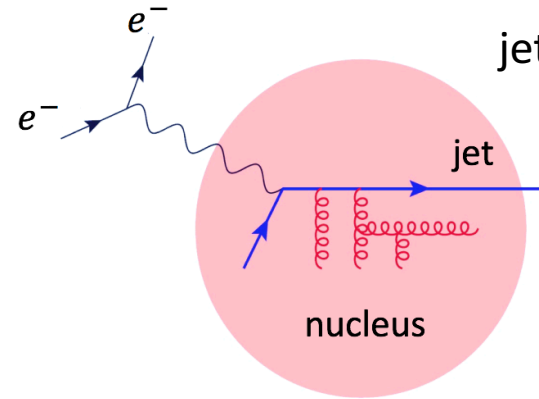
For quark-gluon plasma



J. Casalderrey-Solana and X.-N. Wang,
PRC **77**, 024902 (2008)

JETSCAPE, PRC **104**,
024905 (2021)

For cold nuclear matter



A common relation between
jet energy and x & Q^2 in various processes

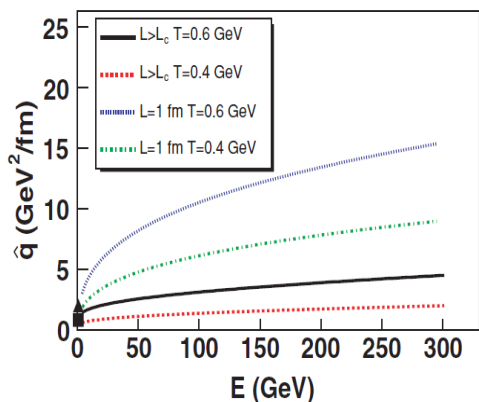
$$E_{\text{jet}} = \frac{Q^2}{2m_p x}$$

(jet energy in nucleus rest frame)

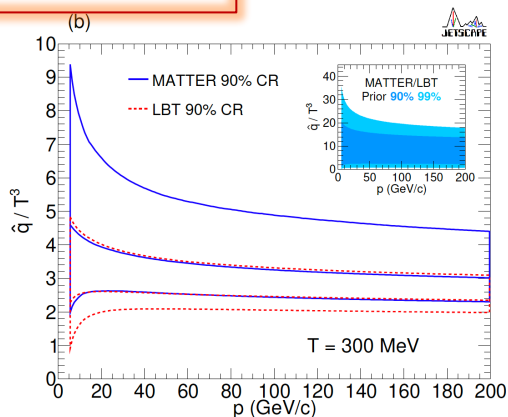
$$\hat{q}(x, Q^2) \rightarrow \hat{q}(E_{\text{jet}}, Q^2)$$

\hat{q} for cold nuclear matter: jet energy dependence

For quark-gluon plasma

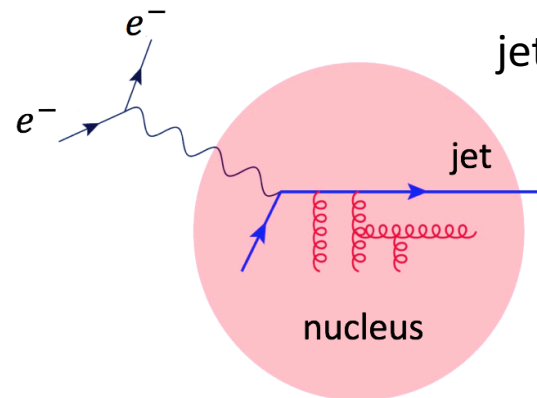


J. Casalderrey-Solana and X.-N. Wang, PRC **77**, 024902 (2008)



JETSCAPE, PRC **104**, 024905 (2021)

For cold nuclear matter

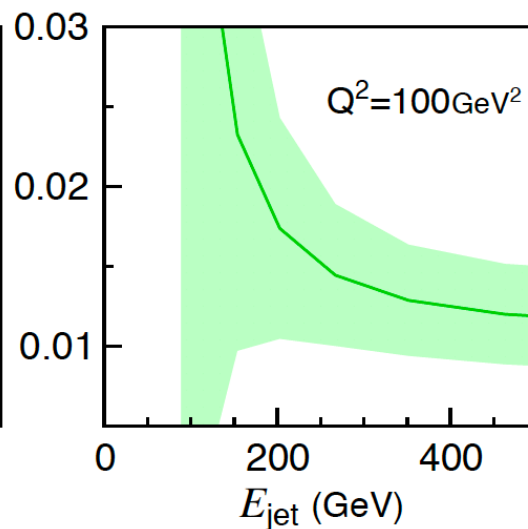
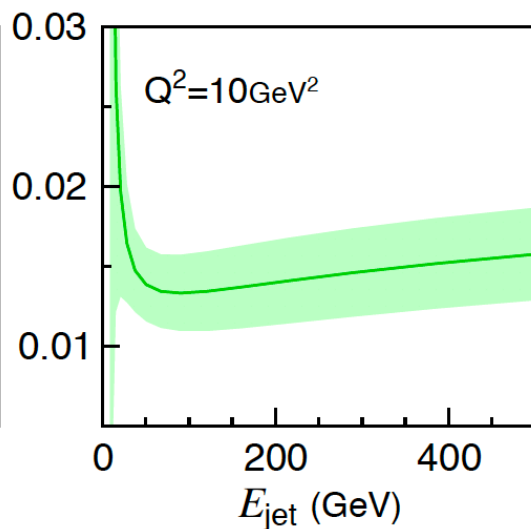
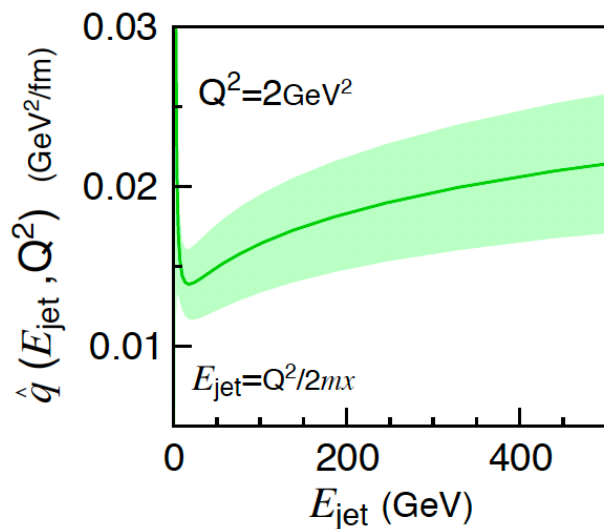


A common relation between jet energy and x & Q^2 in various processes

$$E_{\text{jet}} = \frac{Q^2}{2m_p x}$$

(jet energy in nucleus rest frame)

$$\hat{q}(x, Q^2) \rightarrow \hat{q}(E_{\text{jet}}, Q^2)$$



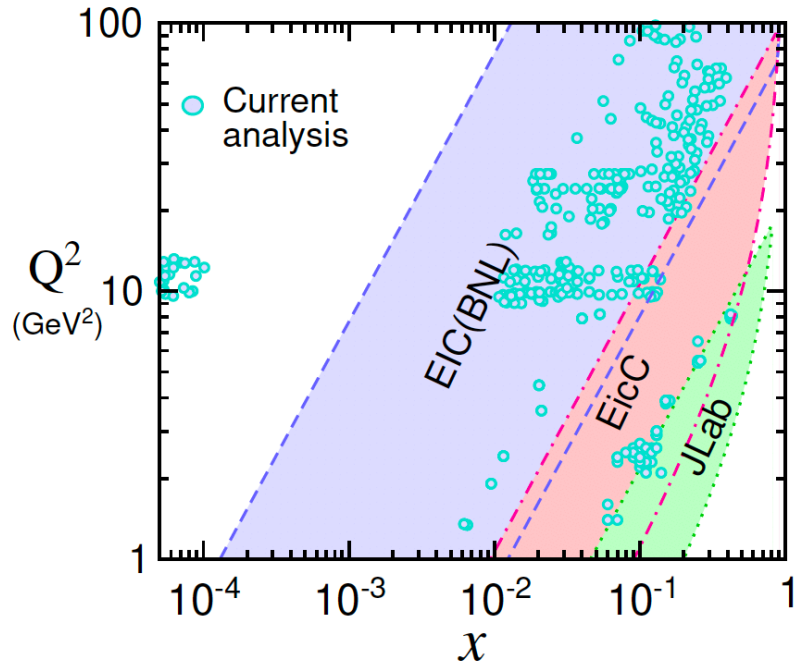
Increasing with jet energy at low Q^2 .

Jet energy dependence is sensitive to resolution scale Q^2 .

How to extend this knowledge to heavy-ion collisions is of interest.

How will EIC deepen our understanding

Kinematics coverage of future EIC facilities

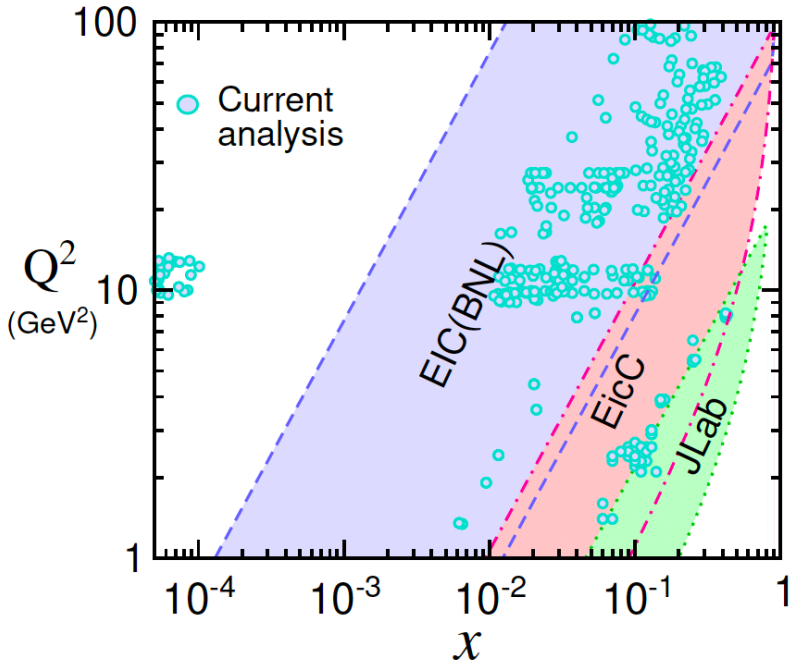


The future EIC experiments, e.g., at EIC (BNL), JLab and EicC (China) will largely extend the coverage of kinematic region and improve the accuracy of the measurement.

PR, Z.B. Kang, E. Wang, H. Xing and B.W. Zhang, 2302.02329

How will EIC deepen our understanding

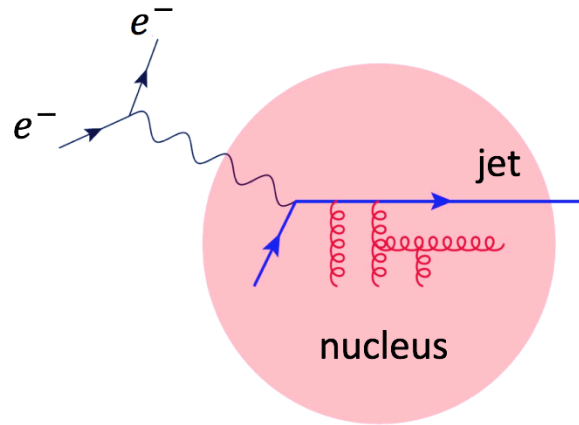
Kinematics coverage of future EIC facilities



The future EIC experiments, e.g., at EIC (BNL), JLab and EicC (China) will largely extend the coverage of kinematic region and improve the accuracy of the measurement.

PR, Z.B. Kang, E. Wang, H. Xing and B.W. Zhang, 2302.02329

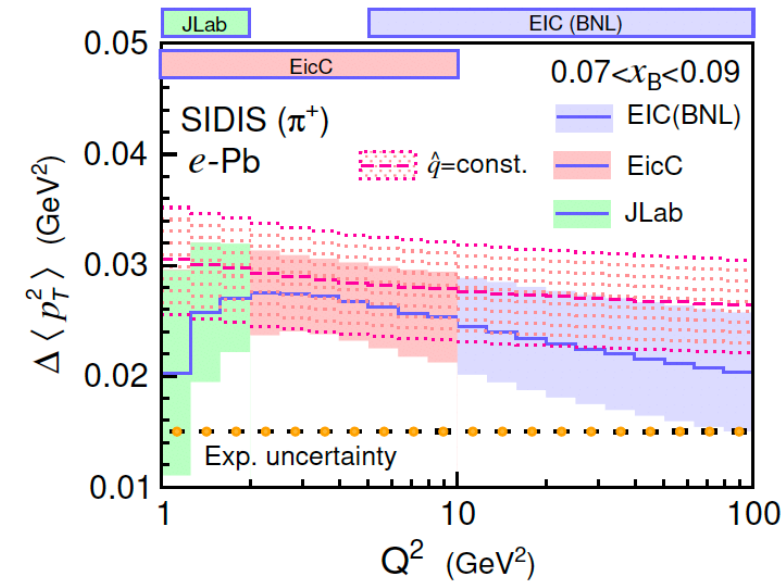
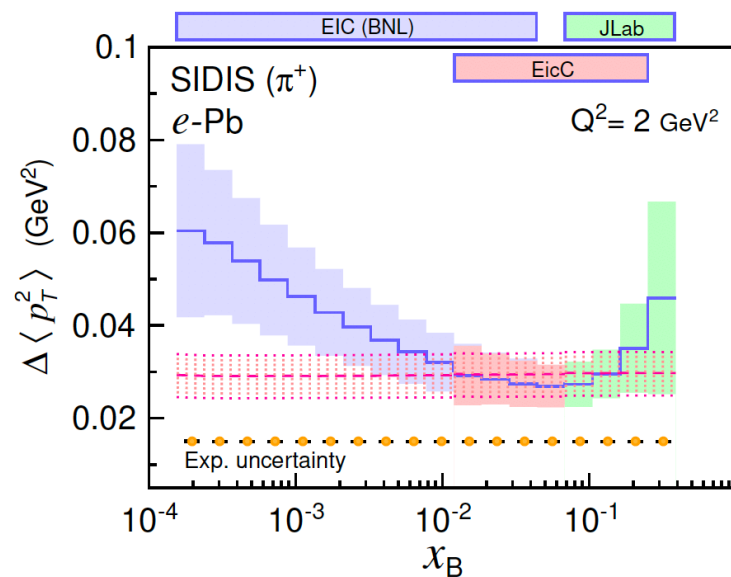
Transverse momentum broadening in SIDID



Abundant yield with nearly full kinematic coverage.

Quark jets dominate.

Imaging $\hat{q}(x, Q^2)$ precisely

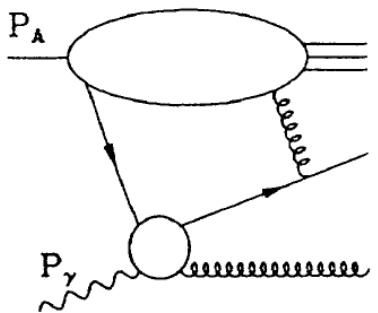


How will EIC deepen our understanding

Nuclear enhancement of transverse momentum imbalance of back-to-back particle pair

H. Xing, Z. B. Kang, I. Vitev and E. Wang, Phys. Rev. D 86, 094010 (2012)

For di-hadron

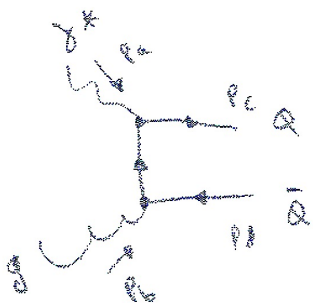


Mainly in mid- and large- x regions.

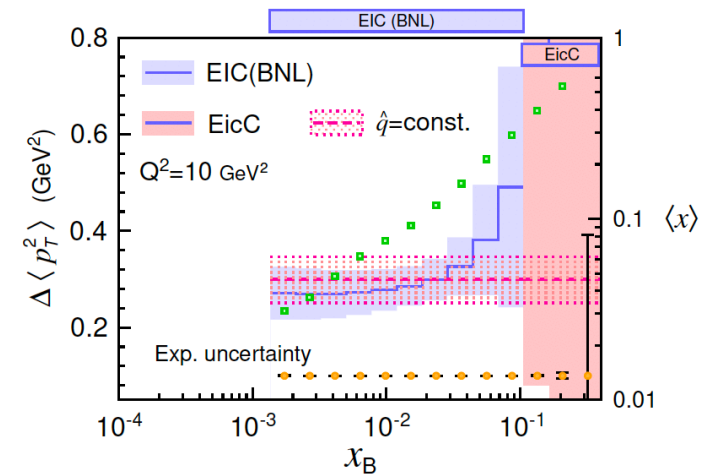
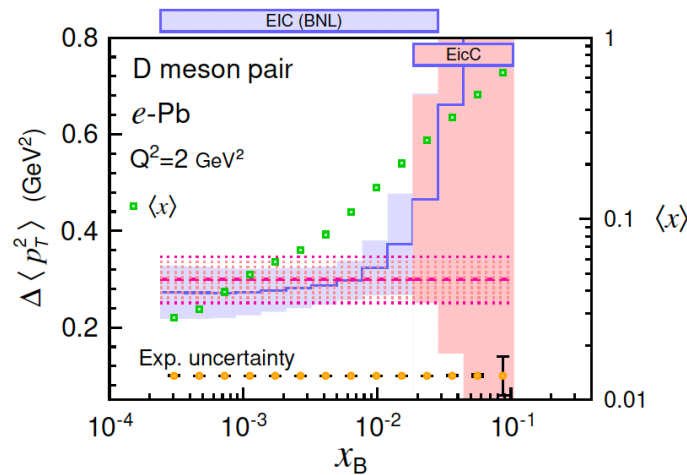
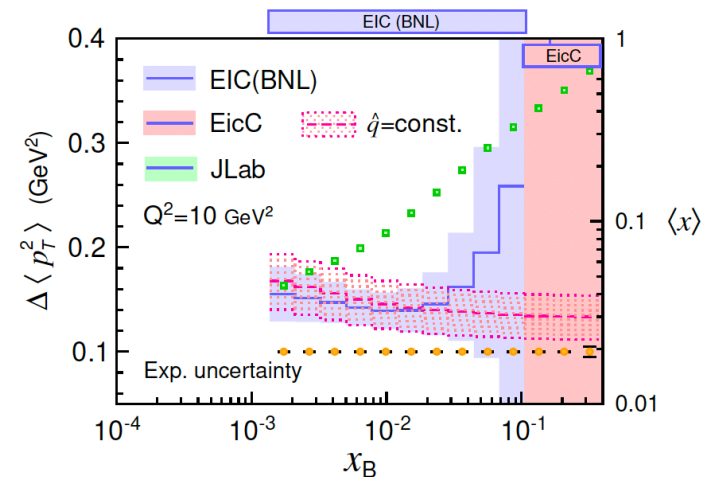
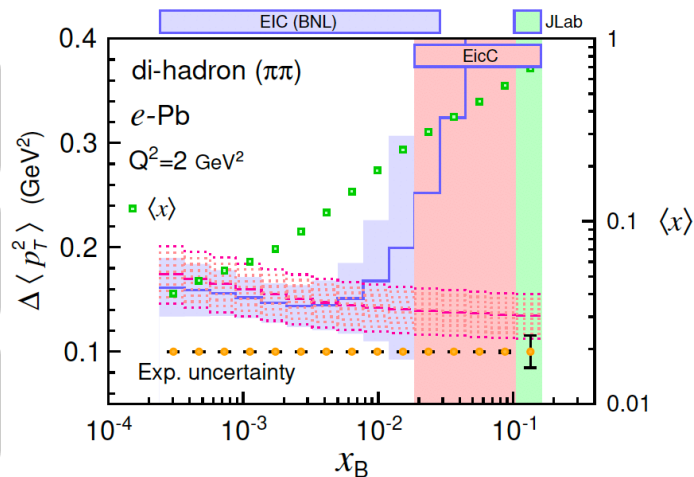
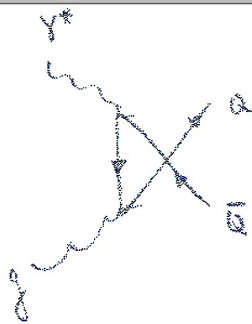
Both quark and gluon jets contribute.

Reducing uncertainties of $\hat{q}(x, Q^2)$ at large- x

For heavy meson pair



Gluon jets dominate.



Summary

1. The possibility to gain the kinematic dependence of \hat{q} in CNM through a global analysis

Similar as the standard PDFs.

2. A universal non-trivial kinematic (x, Q^2) dependence of \hat{q} :

Suggested by current data on transverse momentum broadening.

3. Jet energy dependence of \hat{q} :

May be sensitive to the probing scale.

4. Future EIC experiments in US and China:

Provide a precise image of $\hat{q}(x, Q^2)$

5. $\hat{q}(x, Q^2)$:

Not only useful for jet phenomena, but also the window to nucleus partonic structure (jet tomography).

Thank you!